Cell size regulation in bacteria: a tale of old regulators with new mechanisms

Ezza Khan and Paola E. Mera*

Department of Microbiology, University of Illinois at Urbana-Champaign, Urbana, IL, USA

* Corresponding author e-mail address: pmera@illinois.edu

SUMMARY

Proper function in a bacterial cell relies on intrinsic cell size regulation. The molecular mechanisms underlying how bacteria maintain their cell size remain unclear. The conserved regulator DnaA, the initiator of chromosome replication, is associated to size regulation by controlling the number of origins of replication (*oriC*) per cell. In this study, we identify and characterize a new mechanism in which DnaA modulates cell size independently of *oriC*-copy number. By altering the levels of DnaA without impacting chromosome replication, we demonstrate that DnaA's activity as a transcription factor can slow down cell elongation rate resulting in cells that are ~20% smaller. We identify the peptidoglycan biosynthetic enzyme MurD as a key player of cell size regulation in *Caulobacter crescentus* and in the evolutionarily distant bacterium *Escherichia coli*. Collectively, our findings provide mechanistic insights to the complex regulation of cell size in bacteria.

KEY WORDS. Cell size, DnaA, peptidoglycan, MurD, elongation rate, cytokinesis, *C. crescentus, E. coli*, ppGpp, FtsZ

INTRODUCTION

Across species, bacteria display a diversity of cell shapes, yet within each species, there is a remarkable uniformity in both shape and size (Young, 2006). Maintaining cell size regulation is fundamental for the ability of bacteria to perform basic physiological functions, such as surface transport, biosynthesis, proteome regulation, chromosomal maintenance, and nutrient exchange (Ho & Amir, 2015). For instance, when a cell becomes too large, nutrient transport/utilization can be impacted as transport within the cell is dependent on diffusion (Beveridge, 1988; (Amir, 2014; Grant et al., 2021; Willis & Huang, 2017). Similarly, if a cell becomes too small, it lacks essential volume needed for housekeeping maintenance that can jeopardize the ability to properly segregate their chromosomes (Beveridge, 1988; Willis & Huang, 2017). Regulation of size and shape have also been found to impact virulence (Bartlett et al., 2017; Dalia & Weiser, 2011; Lenski & Travisano, 1994; Salama, 2020; Taylor et al., 2019). *Streptococcus pneumoniae's* ability to reduce its size helps this pathogenic bacterium to circumvent the host immune system (Dalia & Weiser, 2011). Although cell size regulation in bacteria has been intensively studied, the molecular mechanisms involved remain still quite limited.

Bacteria modulate their cell size while orchestrating numerous molecular machineries that temporally and spatially coordinate the replication and segregation of the chromosome with the elongation and constriction of the cell envelope (Westfall & Levin, 2017). One of the conserved regulators of the cell cycle that has been implicated in cell size regulation is the chromosome replication initiator protein, DnaA. DnaA regulates the number of origins of replication (*oriC*) per cell in response to nutrient availability (Boye et al., 1996; Hallgren & Jonas, 2024; Lobner-Olesen et al., 1989). Cells grown in nutrient rich medium (fast growth rates) initiate new rounds of chromosome replication within shorter time intervals and become larger in size compared to cells grown in minimal media (slower growth rates) (Cooper & Helmstetter, 1968; Donachie, 1968). The positive correlation between cell size and *oriC* copy number were reported ~½ century ago (Cooper & Helmstetter, 1968; Donachie, 1968; Helmstetter et al., 1968; Yoshikawa et al., 1964). Since then, many studies have been reported supporting and rejecting the role of chromosome replication initiation with cell size regulation in bacteria (Bates & Kleckner, 2005; Boye et al., 1996; Churchward et al., 1981; Hill et al., 2012; Koppes et al., 1980; F. Si et al., 2017; Wold et al., 1994; Zheng et al., 2020; Zheng et al., 2016). An emerging insight is that the regulation of bacterial cell size is not controlled by a single trigger, but rather by a complex and multifactorial process (Jun et al., 2018).

As the regulator of chromosome replication initiation, DnaA plays an essential role in maintaining genome integrity and in ensuring the survival of the bacterial cell. DnaA bound to ATP oligomerizes at the origin of replication (*oriC*), opens *oriC*, and recruits the replication machinery to initiate chromosome replication (Hansen & Atlung, 2018; Kohiyama, 2020). Besides its role in chromosome replication, DnaA also serves as a conserved transcription factor (Menikpurage et

al., 2021; W. Messer & C. Weigel, 1997), albeit fewer mechanistic details are known about this function. DnaA is composed of four structural and functional domains (domains I – IV). The N-terminal domain (domain I) is involved in protein-protein interactions, and it is connected to the AAA+ ATPase domain (domain III) by a helical linker domain (domain II) (Duderstadt & Berger, 2013; Fujikawa et al., 2003). The DNA-binding domain (domain IV) can bind either at *oriC* and initiate chromosome replication or bind at promoter regions and regulate transcription (Hansen et al., 1982). The ability to bind/hydrolyze ATP is essential for DnaA's activity as a replication initiator (Mizushima et al., 1996; Sekimizu et al., 1987). The nucleotide bound (ATP vs. ADP) also modulates DnaA's activity as a transcription factor (Fernandez-Fernandez et al., 2011; Olliver et al., 2010; Speck et al., 1999).

The diderm oligotrophic bacterium *Caulobacter crescentus* is known as an excellent model to study cell cycle regulation, including cell size regulation (Banerjee et al., 2017; Barrows & Goley, 2023; Campos et al., 2014; Govers & Jacobs-Wagner, 2020; Lambert et al., 2018). Upon cell division, *C. crescentus* produces two genetically identical but morphologically distinct cells: a smaller motile swarmer cell that cannot initiate chromosome replication and a sessile stalk cell that is replication competent (Barrows & Goley, 2023) (Figure 1A). The dimorphic life cycle of *C. crescentus* enables isolation of homogeneous populations of cells at different developmental stages (Ardissone et al., 2014; Evinger & Agabian, 1977; Schrader & Shapiro, 2015; Stove & Stanier, 1962). Recently, swarmer cells and stalk cells were shown to grow at different rates despise sharing identical genomes and environments (S. Glenn et al., 2024; T. W. Ng et al., 2024). *C. crescentus* initiates chromosome replication once per cell cycle regardless of nutrient conditions (Marczynski, 1999), which facilitates the analysis of *oriC* copy number per cell size. The genetic circuit that regulates the forward progression of the cell cycle has been extensively characterized in *C. crescentus* revealing that each transcription factor in the circuit regulates each other's expression leading to oscillating abundance of global regulators (J. Collier et al., 2006; Kirkpatrick & Viollier, 2012). DnaA is one of the master transcription factors that make up this genetic circuit (Justine Collier et al., 2006; A. K. Hottes et al., 2005).

In this study, we identify and characterize a new mechanism of DnaA's regulation of cell size that is independent of *oriC*-copy number. We found that increasing the cellular levels of DnaA 3-fold (referred here as 3x-DnaA cells) results in a reduction of cell size by ~20% without impacting chromosome replication. This effect of DnaA on cell size is independent of parameters previously implicated with cell size regulation, like protein synthesis and the alarmone ppGpp molecule. Our transcriptional and mutant analyses revealed that DnaA's activity as a transcription factor is involved in the regulation of cell size. 3x-DnaA cells display increased expression of genes involved in cell wall biosynthesis, including the conserved *murD* and *mraY*. The increased expression *murD* alone results in cells displaying a reduced cell size irrespective of media type (rich and minimal). We discovered that this connection between *murD* and reduction in cell size is conserved in the evolutionary diverse bacterium *E. coli.* After analyzing multiple cell cycle

97 parameters, our data revealed that the only parameter that changed in 3x-DnaA small cells
98 compared to WT cells is the rate of cell elongation. In fact, elongation rate slowed down also by
99 ~20% consistent with a similar percent reduction in cell size and consistent with cell wall
100 biosynthesis being involved.

101 **RESULTS**

102 *DnaA levels impact cell size independent of oriC copy number*

103 A common strategy to study the essential protein DnaA is to use constructs where the native *dnaA*
104 gene is knockout and a *dnaA* copy is engineered to be expressed from inducible promoters. While
105 characterizing such constructs, we noticed that cells expressing *dnaA* from the inducible promoter
106 vanillate (*dnaA*::Ω, P_{van}-*dnaA*) are smaller compared to wildtype cells with *dnaA* at its native locus
107 (Figure 1B). This DnaA-dependent reduction in cell size was only present when cells were grown
108 in minimal media (M2G) but not in nutrient rich media (PYE). The quantification of cell size
109 revealed that in minimal media cell length decreased ~20 % whereas the width remained the
110 same (Figure 1CD). The observed changes only in length are consistent with previous reports
111 showing that *C. crescentus* regulates its size by modulating the cell length (Campos et al., 2014).
112 To ensure that this effect was not in response to the inducer vanillate, we analyzed the cell size
113 of cells expressing *dnaA* from the other commonly used promoter, P-xylose (Thanbichler et al.,
114 2007). Our data revealed that cells expressing *dnaA* from either inducible promoter displayed the
115 same reduction in cell size when grown in minimal media (Supplemental Figure 1A).

116 Given that DnaA initiates replication at *oriC* and *oriC* copy number are correlated with cell size
117 (Moselio Schaechter et al., 1958), we examined the possibility that changes in *oriC* copy number
118 caused the change in cell size. In *C. crescentus*, replication initiates only once per cell cycle
119 resulting in cells with one or a maximum of two *oriC* copies (Marczynski, 1999). To quantify *oriC*
120 copy number, we used the centromere-like region *parS* (~8 kilobases away from *oriC*) as proxy
121 of number of origins of replication (Thanbichler & Shapiro, 2006; Toro et al., 2008). We
122 fluorescently labeled the *parS*-binding protein ParB and tracked the number of CFP-ParB foci.
123 Our data showed that cells expressing *dnaA* from inducible promoters (*dnaA*::Ω, *parB::cfp-parB,*
124 $P_{van\ or\ xyl}$-*dnaA*) displayed wildtype numbers of *oriC* copies per cell (Figure 1E), discarding the
125 possibility that changes in *oriC* copy number are responsible for the effect on cell length.
126 Consistent with no alteration in *oriC* copy number, cells expressing *dnaA* from inducible promoters
127 grew at similar doubling rates as wildtype cells in rich or minimal media (Figure 1F)

128 Taking advantage of *C. crescentus* asymmetric cell cycle, we examined whether the DnaA-
129 dependent impact on cell length was specific to the developmental stage of the cell. We wondered
130 about this possibility based on the recent findings that *C. crescentus* shows differential growth
131 rates through their cell cycle (Skye Glenn et al., 2024; Tin Wai Ng et al., 2024). To test this
132 hypothesis, we analyzed cell size of isolated homogeneous population of swarmer cells (Evinger
133 & Agabian, 1977; Schrader & Shapiro, 2015). Our analysis revealed that swarmer cells and

134 stalked cells display a similar ~20% reduction in cell length (Figure 1G) demonstrating that the
135 impact on cell size is not specific to the developmental stage of the cell. Collectively, these data
136 revealed that changing *dnaA's* transcriptional regulation result in a reduction of cell length
137 independent of both *oriC* copy number and cell cycle stage.

138

139 *Cell length decreases as DnaA levels increase*

140 The levels and activity of DnaA as a replication initiator are regulated at a multitude of levels,
141 including post-transcriptionally and post-translationally (Felletti et al., 2019; Katayama et al.,
142 2010). In *C. crescentus*, the DnaA levels are 3- to 4-fold higher when grown in rich media than in
143 minimal media (Justine Collier et al., 2006; Frandi & Collier, 2019; Jared M Schrader et al., 2016).
144 Given that our observed reduction in cell length was linked to *dnaA*'s transcriptional regulation
145 (native vs. inducible promoter), we examined whether the levels of the protein DnaA had changed
146 when expressed from inducible promoters. Using western blot analysis with antibodies specific to
147 DnaA, we found that the small cells (*dnaA*::Ω, *parB::cfp-parB,* $P_{van\ or\ xyl}$-*dnaA*) grown in minimal
148 media display ~3-fold higher levels of DnaA compared to wildtype grown under the same condition
149 (Figure 2A). In rich media, however, we observed no differences in DnaA levels between wildtype
150 and cells expressing *dnaA* from inducible promoters. These data suggested that the levels of
151 DnaA protein, and not necessarily the type of media, were the cause of the change in cell size.

152 To evaluate our hypothesis that elevated DnaA levels contribute to the observed reduction in cell
153 length, we sought to identify conditions that would increase DnaA levels in cells cultured in
154 nutrient-rich media. To increase the levels of DnaA, we constructed two chromosomal *dnaA*
155 merodiploid strains: one with *dnaA* under its native locus plus a copy under an inducible promoter
156 (P_{van}-*dnaA*) or a strain with two copies of *dnaA* under two different inducible promoters (P_{van}-*dnaA*
157 P_{xyl}-*dnaA*). The quantification of DnaA levels with western blots revealed that none of the
158 chromosomal *dnaA* merodiploid strains grown in rich media produced higher levels of DnaA than
159 wildtype. To achieve higher levels of *dnaA* overexpression, we constructed a *C. crescentus* strain
160 with *dnaA* overexpressed from a replicating plasmid. Considering that this approach can lead to
161 over-initiation of chromosome replication, we induced expression of *dnaA* for only ~2 cell cycles
162 in rich media (3h induction). Using western blots, we confirmed that 3h induction results in ~3-fold
163 higher DnaA levels compared to wildtype (Supplementary Figure 2A). However, even under this
164 short-term induction, we observed a significant percent of cells (>10%) over-initiated chromosome
165 replication (Supplementary Figure 2B). To avoid the implications that over-initiation of
166 chromosome replication has on cell size, we continued our analysis using only chromosomal
167 inducible promoters and only minimal media as the growth condition. Later in this manuscript, we
168 revisit rich media as a variable of cell size.

169 Having determined the upper limits of DnaA levels in minimal media that maintain the normal 1-2
170 *oriC* copies per cell, we next examined whether the changes in cell length are proportional with
171 the cellular levels of DnaA. We used western blot analysis to first confirm that increasing levels of

172 inducer correlated with increasing levels of DnaA (Figure 2B). Notably, as the levels of DnaA
173 increased, we observed a corresponding decrease in cell length (Figure 2C). We were able to
174 reach the highest expression levels of DnaA (without over-initiation of replication) when cells were
175 grown with the inducer xylose as the sole carbon source (no glucose added since glucose can
176 inhibit the xylose promoter (Stephens et al., 2007)). Consistent with our hypothesis, our analysis
177 showed that the highest DnaA concentration also results in the highest decrease in cell length in
178 cells grown in minimal media (Figure 2D). Collectively, these data demonstrate that increases in
179 DnaA levels, without impacting replication initiation, linearly correlate with decreases in cell length.

180

181 *Rate of lateral cell growth is slower in small cells compared to wildtype*

182 We next determined how cells expressing 3x-DnaA levels became smaller. For simplicity, we will
183 refer to cells expressing *dnaA* from an inducible promoter grown in minimal media as 3x-DnaA
184 cells. *C. crescentus*, like most rod-shaped bacteria, undergo different growth phases over the cell
185 cycle: pure elongation phase where new PG is inserted along the lateral walls followed by the
186 zonal phase, where new PG is added at the division site (Aaron et al., 2007). Thus, we
187 hypothesized that 3x-DnaA cells' reduction in size was due to slower cell growth, faster
188 constriction rate, or a combination of both scenarios. To test this hypothesis, we imaged
189 synchronized 3x-DnaA cells (*dnaA*::Ω, *parB::cfp-parB,* P_{van}*-dnaA*) and wildtype cells over time
190 through one complete cell cycle starting from the G1 phase (swarmer state) through the
191 completion of cytokinesis. Each individual cell was then analyzed through the progression of its
192 cell cycle using an automated analysis with the Fiji plugin MicrobeJ (Ducret et al., 2016;
193 Schindelin, Arganda-Carreras, Frise, Kaynig, Longair, Pietzsch, Preibisch, Rueden, Saalfeld,
194 Schmid, et al., 2012). We calculated for each cell the rates of cell growth and the rates of
195 constriction (Mahone et al., 2024). Our data revealed that the constriction rate remained the same
196 in 3x-DnaA small cells compared to wildtype cells (Figure 3AB). Unlike constriction rate, we
197 discovered that 3x-DnaA small cells elongate at a rate ~20% slower than wild-type cells (Figure
198 3AC). These exciting results correspond to the observed ~20% reduction in cell length in 3x-DnaA
199 cells.

200

201 *Cell size determinants and their connection to DnaA.*

202 Numerous factors have been reported to positively influence bacterial cell size, although the
203 precise molecular mechanisms underlying these regulations has remained elusive. We
204 investigated whether the observed DnaA-dependent effect on cell length is connected to
205 previously reported determinants of cell size in bacteria. For instance, reducing the total protein
206 content in the cell has been shown to correlate with a reduction in cell size (Basan et al., 2015).
207 In *B. subtilis,* reducing the synthesis of proteins (using subinhibitory levels of the ribosome
208 targeting antibiotic chloramphenicol) results in ~10% cell length reduction without changes in cell

209 width (Vadia et al., 2017). Analogous to *B. subtilis*, our analysis of wildtype *C. crescentus* cells
210 exposed to sub-lethal concentrations of chloramphenicol revealed a reduction in cell length by
211 approximately 10%, while cell width remained unchanged (Figure 3D). Notably, the already small
212 3x-DnaA cells became even smaller by approximately 10% when exposed to chloramphenicol
213 compared to the no antibiotic condition (Figure 3D). These results revealed that DnaA's effect on
214 cell size is independent from the effect that protein content has on cell size regulation. The
215 influence of chloramphenicol on the curvature of *C. crescentus* (Cabeen et al., 2009) remained
216 unchanged in 3x-DnaA cells compared to wildtype (Supplemental Figure 3A).

217 The alarmone molecule guanosine tetra- or pentaphosphate (p)ppGpp, a global inhibitor of
218 biosynthesis, has been implicated in cell size in various bacterial species. The cellular levels of
219 (p)ppGpp are regulated by the Rsh family enzymes RelA & SpoT (Srivatsan & Wang, 2008;
220 Tozawa & Nomura, 2011). Unlike *E. coli* and *B. subtilis*, *C. crescentus* and other
221 alphaproteobacterial species only encode the SpoT-dependent pathway (Wells & Long, 2002) In
222 *E. coli*, levels of (p)ppGpp have been shown to impact cell size upon amino acid starvation (Traxler
223 et al., 2008). In *C. crescentus*, artificially increasing the levels of (p)ppGpp by expressing a
224 constitutively active RelA from *E. coli* results in cells with decreased cell size (Gonzalez & Collier,
225 2014). To examine whether DnaA's impact on cell length was connected to levels of (p)ppGpp,
226 we constructed a mutant strain unable to synthesize (p)ppGpp by knocking out the gene encoding
227 the bifunctional (p)ppGpp synthetase/hydrolase SpoT. Our analysis revealed that wildtype cells
228 with and without *spoT* retained the same cell size (Figure 3E). Similar to wildtype cells, 3x-DnaA
229 cells with or without *spoT* display the same cell size demonstrating that the alarmone molecule
230 (p)ppGpp is not connected to the observed DnaA-dependent change in size.

231 The biosynthesis of fatty acid and cell wall have also been implicated with cell size regulation. To
232 examine whether fatty acid and peptidoglycan (PG) biosynthesis were linked to the reduction in
233 size of 3x-DnaA cells, we followed established protocols to obstruct their biosynthesis using sub-
234 lethal concentrations of the antibiotics cerulenin and Fosfomycin. Cerulenin inhibits the first
235 condensation reaction between acetyl-CoA and malonyl-acyl-carrier-protein catalyzed by FabH
236 (b-ketoacyl-acyl-carrier protein synthase) (Cronan, 2014). In *B. subtilis* and *E. coli*, exposure to
237 cerulenin result in ~10% reduction in cell length (Fangwei Si et al., 2017; Vadia et al., 2017).
238 Unfortunately, we are unable to make any conclusions about cerulenin because we found that the
239 viability of *C. crescentus* is highly sensitive to even low levels of cerulenin (Supplemental Figure
240 3B). One potential explanation to this high sensitivity is that *C. crescentus* encodes a single copy
241 of FabH whereas *B. subtilis* has two FabH homologs FabHA and FabHB (Kaneda, 1991; Yao et
242 al., 2012). Regarding PG biosynthesis, Fosfomycin is used to inhibit the first committed enzyme,
243 MurA (UDP-N-acetylglucosamine enolpyruvyl transferase) (Typas et al., 2012). Fosfomycin
244 exposure in wildtype *C. crescentus* cells has been reported to cause cells to increase length and
245 width (Harris & Theriot, 2016; Irnov et al., 2017). When we analyzed wildtype cells exposed to
246 similar levels of Fosfomycin (5 μg/mL), we found that indeed cells become bigger in length and
247 width (Supplemental Figure 3C). However, our analysis of *oriC* copy number in both wildtype and

248 3x-DnaA cells exposed to Fosfomycin revealed that these larger cells over-initiate chromosome
249 replication resulting in abnormal >2 *oriC* copies per cell (Supplemental Figure 3D). Because we
250 cannot resolve whether multiple *oriC* copies caused the cell size increase or cell size increase
251 caused the over-initiation of chromosome replication, we cannot make any conclusions based on
252 these data about the potential connection between DnaA and PG biosynthesis. Based on these
253 analyses of known determinants of cell size regulation in bacteria, our data revealed that protein
254 synthesis and (p)ppGpp are not connected to the reduction in size of 3x-DnaA cells. We will revisit
255 PG biosynthesis later in this manuscript.

256

257 *DnaA requires binding to both ATP & DNA to exert impact on cell length*

258 To gain insights into the mechanism of how DnaA influences cell size, we examined the role of
259 the various domains of this master regulator (Figure 4A) by constructing a set of variants that
260 included truncations or amino acid modifications targeting these domains. Because DnaA is
261 essential and minor modification to any of these domains can impact viability, we analyzed the
262 effects on cell size using merodiploid strains. These merodiploid strains express variants of DnaA
263 from an inducible chromosomal promoter (P_{xyl}) while the native copy of *dnaA* remains intact. Our
264 data revealed that this type of constructs with wildtype *dnaA* expressed from *Pxyl* (P_{xyl}-*dnaA*) also
265 display the ~20% reduction in cell length when DnaA levels are increased ~3-fold (Figure 4C,
266 Supplemental Figure 4A). We confirmed that the expression of DnaA variants from P_{xyl} had no
267 dominant negative effect on viability using colony forming units (CFU) (Figure 4B). Presence of
268 protein variants compared to empty vector control (EV) was confirmed with western blots (Figure
269 4C).

270 In *C. crescentus*, an alanine-rich region at the N-terminal end of domain I is involved in the
271 regulation of cellular levels of DnaA upon nutrient starvation (Felletti et al., 2021). We reasoned
272 that if this ala-rich domain was involved in triggering the change in cell size, increasing the levels
273 of a truncated version of DnaA missing this alanine rich region would have no effect on cell length.
274 However, cells expressing a truncation of the alanine rich region expressed from P_{xyl} (referred as
275 ∆ala) retained their ability to reduce their cell length (Figure 4D), albeit to marginally lower levels.
276 The small difference in cell length reduction (~18% vs. ~22%) can be attributed to lower levels of
277 expression of this variant compared to cells with 3x-wildtype-DnaA (Figure 4C). These data further
278 support that the impact on cell length is dependent on DnaA levels, and that the alanine rich N-
279 terminal domain is not responsible in DnaA's regulation of cell length.

280 We considered another possibility were DnaA's role with cell size regulation was independent of
281 its ability to bind DNA. We posit that DnaA itself could regulate cell size potentially by directly
282 modulating the activity of cell size regulators independent of DNA binding. We tested this
283 hypothesis by analyzing the effect on cell length from a DnaA variant with the DNA-binding domain
284 (domain IV) truncated (referred as ∆IV). Expression of this DNA-binding variant had no effect on
285 cell length compared to wildtype levels of DnaA (Figure 4D), revealing that DnaA's ability to bind

286 DNA is required for its role with cell size regulation. Wondering whether ATP binding and/or
287 hydrolysis was required for DnaA's impact on cell length, we analyzed a variant with a single
288 amino acid substitution that interrupts ATP binding. We did not analyze DnaA variants unable to
289 hydrolyze ATP because such variants are stuck in the active form and over-initiate chromosome
290 replication, which would inevitably impact cell size in an *oriC* copy dependent manner. We
291 constructed DnaA-K195I, a variant encoding a mutation in the Walker A box that affects DnaA's
292 ability to bind ATP (Mizushima et al., 1998). Our data revealed that DnaA-K195I lost the effect on
293 cell length and cells expressing this variant displayed wildtype cell size (Figure 4D).

294 Collectively, the analyses of DnaA variants revealed that DnaA requires to bind DNA and to bind
295 ATP to cause the effect on cell size. Given that DNA-binding and ATP-binding are involved in
296 regulating both functions of DnaA (chromosome replication initiator and transcription factor), we
297 set out to differentiate DnaA's effect on cell length between these two functions. Because we
298 cannot uncouple these two functions without altering the proper progression of the cell cycle and
299 thus cell size regulation, we proceeded by analyzing each function independently.

300

301 *Chromosome replication remains unchanged in 3x-DnaA small cells*

302 The initiation of chromosome replication requires DnaA-ATP oligomerization at *oriC*, which opens
303 the double stranded DNA allowing for components of the replisome to assemble and to initiate
304 replication bidirectionally (Leonard & Grimwade, 2011). We explored the possibility that 3x-DnaA
305 levels could alter the overall process of chromosome replication, potentially leading to the
306 reduction in cell size. To test this hypothesis, we used time-lapse microscopy to image
307 synchronized swarmer cells throughout their cell cycle, focusing on three key events of
308 chromosome replication: (a) timing of replisome assembly, (b) timing of replication initiation, and
309 (c) progression of the replication forks (Figure 5). To track replisome assembly, we imaged a
310 strain encoding the replisome component DnaN (β-clamp) fluorescently tagged at *dnaN's* native
311 chromosomal locus (Collier & Shapiro, 2009; Jensen et al., 2001). Our analysis of the time when
312 the DnaN-mCherry focus emerges revealed that the 3x-DnaA small cells and wildtype cells
313 assembled their replisomes at similar times (Figure 5A). To determine timing of replication
314 initiation, we tracked the appearance of two *parS* loci (8kb from *oriC*) using the *parS*-binding
315 protein CFP-ParB (Toro et al., 2008). Our data revealed the 3x-DnaA small cells initiate
316 chromosome replication at similar times as wildtype cells (Figure 5B). Lastly, we examined
317 replisome progression by comparing when a chromosomal locus near the gene *pleC* (1.3 Mb from
318 *oriC*) is replicated. To track replication of *pleC*, we used a strain engineered to encode the Yersinia
319 pestis sequence of *parS(*pMT1) near the *pleC* locus and the corresponding ParB(pMT1)
320 fluorescently labelled expressed from an inducible promoter (Schwartz & Shapiro, 2011). We
321 included to this strain a fluorescent tag with the *C. crescentus'* native ParB as an internal control.
322 Analyzing the timing of replication of *parS* and *pleC* revealed no difference between wildtype and

323 3x-DnaA small cells (Figure 5C). Overall, these data indicate that the higher levels of DnaA in 3x-
324 DnaA small cells do not alter the overall process of chromosome replication.

325

326 *Small cells display changes in transcriptional profiles*

327 After demonstrating that 3x-DnaA levels do not affect the progression of chromosome replication,
328 we proceeded to investigate DnaA's other conserved role as a master transcriptional regulator.
329 (Alison K. Hottes et al., 2005; Walter Messer & Christoph Weigel, 1997; Washington et al., 2017).
330 In *C. crescentus*, the DnaA transcriptional regulon includes genes encoding components of the
331 replisome, cell cycle regulators, and nucleotide biosynthesis (A. K. Hottes et al., 2005). We
332 hypothesized that DnaA regulates cell size through its activity as a transcription factor. To test
333 this hypothesis, we examined whether the levels of the transcriptional regulon of DnaA changed
334 in 3x-DnaA small cells. For these analyses, we used the *dnaA* merodiploid strains to enable
335 comparisons with the DnaA variants. When comparing 3x-DnaA (P_{xyl}-*dnaA*^{WT}) with an empty-
336 vector control, our RNA-Seq analysis revealed relatively few genes change expression: 45 total
337 genes with 35 upregulated and 10 downregulated (≥1.5-fold change and FDR<0.05)
338 (Supplemental Table 1). To further exclude non-contributing factors responsible for changes in
339 cell length, we compared RNA-Seq changes between P_{xyl}-*dnaA*^{WT} cells (exhibiting reduced size)
340 and P_{xyl}-*dnaA-K195I* (displaying unaffected cell size). Using this strategy with the same
341 parameters of ≥1.5-fold change and FDR<0.05, our list of potential genes was reduced to 23
342 (Table 1). From this list we focused on genes involved in cell cycle progression. To validate our
343 hits, we used constructs with chromosomal merodiploid strains to circumvent the high expression
344 levels associated with replicating plasmids, given that the genes of interest exhibited changes of
345 less than 2-fold.

346 The 1.5-fold increase in expression of the *ftsZ* gene in 3x-DnaA cells (*parB::cfp-parB*, P_{xyl}-*dnaA*^{WT})
347 cells immediately stood out for multiple reasons (Figure 6A): *ftsZ* is part of the transcriptional
348 regulon of DnaA (Alison K. Hottes et al., 2005); the transcriptional regulation of *ftsZ* is dependent
349 on the nucleotide-bound to DnaA (Fernandez-Fernandez et al., 2011); and FtsZ is a key regulator
350 of the divisome, the molecular machinery that drives cytokinesis and cell wall biosynthesis at the
351 septum (Sackett et al., 1998), both functions that can directly impact cell size. To characterize the
352 potential role of FtsZ, we examined whether the levels of the FtsZ protein were higher in 3x-DnaA
353 cells compared to empty vector, like our transcriptomics data suggested. Using western blots with
354 FtsZ specific antibodies (gift from Erin Goley's Lab), our data revealed no clear differences in FtsZ
355 levels (Figure 6B). To further characterize whether elevated levels of FtsZ lead to a reduction in
356 cell size, we constructed a chromosomal *ftsZ* merodiploid strain (*parB::cfp-parB*, P_{xyl}-*ftsZ*) that
357 displayed increased levels of FtsZ (Supplementary Figure 6A). Our data revealed that increasing
358 FtsZ levels does not decrease cell length. Instead, cells with increased FtsZ levels retain similar
359 size as wildtype but they generate mini-cells (Figure 6C, Supplementary Figure 6B), consistent
360 with previous reports (Goley et al., 2010). These data demonstrate, that FtsZ is not the key player

361 in the reduction of cell size in 3x-DnaA cells. No changes in FtsZ protein levels in 3x-DnaA cells
362 are consistent with our findings that these small cells display no changes in their constriction rate
363 (Figure 3B).

364 Another notable gene within DnaA's transcriptional regulon is *gcrA*, which exhibited a 1.8-fold
365 increase in 3x-DnaA cells (Figure 6A). This gene encodes for the master transcription factor GcrA
366 (Justine Collier et al., 2006). GcrA regulates the transcription of ~200 genes, many of which are
367 critical in the progression through the S-phase and later stages of the cell cycle (Haakonsen et
368 al., 2015). To test whether increased levels of GcrA cause cells to reduce their cell length, we
369 constructed a *gcrA* chromosomal merodiploid strain (*parB::cfp-parB,* P_{xyl}*-gcrA*). Increased
370 expression of the master transcription factor GcrA resulted in cells with longer cell length, instead
371 of shorter (Figure 6C,D), consistent with previous reports (Haakonsen et al., 2015; Holtzendorff
372 et al., 2004).

373 We next explored an alternative hypothesis where DnaA regulates cell size indirectly through the
374 transcriptional regulon of GcrA. From our list of 23 genes, we focused on three genes that are
375 part of the GcrA regulon and are conserved in bacteria: *dnaG* (+1.8-fold) involved in DNA
376 replication, *murD* (+1.5-fold) and *mraY* (+1.6-fold) involved in PG biosynthesis. The DNA primase
377 DnaG represented an interesting target to regulate cell size because DnaG directly regulates the
378 rate of DNA replication in a ppGpp-dependent manner (Levine et al., 1991; Maciag et al., 2010).
379 To test DnaG's potential role with cell size regulation, we analyzed a *dnaG* chromosomal
380 merodiploid strain (*parB::cfp-parB,* P_{xyl}*-dnaG*) and found that induction of *dnaG* results in no
381 changes in cell size (Figure 6CD). These results are consistent with our findings that ppGpp and
382 the overall process of DNA replication are not involved in the cell size reduction of 3x-DnaA cells.

383 Peptidoglycan biosynthesis plays a critical role in the regulation of cell size given that it directly
384 facilitates the expansion of the cell envelope during cell growth and during constriction at the
385 division plane (Aaron et al., 2007). MurD is one of the four cytoplasmic ATP-dependent enzymes
386 that catalyze the successive additions of amino acids to UDP-N-acetylmuramic acid in PG
387 biosynthesis (Typas et al., 2012). MraY transfers UDP-N-acetylmuramic acid-pentapeptide onto
388 the lipid carrier bactoprenol forming the intermediate known as lipid I (Ikeda et al., 1991). To test
389 the hypothesis that changes in MurD and/or MraY levels were responsible for the changes in cell
390 size observed in 3x-DnaA small cells, we constructed chromosomal merodiploid strains of each
391 to titrate the levels of these proteins using wildtype as the parent strain. Induction of *mraY*
392 expression in the merodiploid strain (*parB::cfp-parB,* P_{xyl}*-mraY*) did not reduce cell length but
393 instead caused a subtle but significant increase in cell length compared to empty vector (Figure
394 6C,D). Excitingly, analysis of the *murD* merodiploid strain (*parB::cfp-parB,* P_{xyl}*-murD*) revealed
395 that induced expression of *murD* results in cells with ~10% reduction in cell size (Figure 6D).

396 *MurD as a key player of cell size independent of growth media*

397 Altering the expression of *murD* was the only genetic modification from our RNA-Seq analysis
398 that led to a decrease in cell size. Wondering whether we could achieve an even greater reduction
399 in cell size by further increasing *murD* expression beyond the already higher levels in 3x-DnaA
400 cells, we constructed a *murD* merodiploid strain using the 3x-DnaA cells as the parent strain
401 (*parB::cfp-parB, dnaA*::Ω, P_{van}-*dnaA*, P_{xyl}-*murD*). Our data revealed that indeed, induction of *murD*
402 overexpression in the 3x-DnaA cells results in an additional ~10% decrease in cell length (Figure
403 7A). However, the higher induction of *murD* in 3x-DnaA cells and/or their smaller cell size led to
404 a defect on growth rate (Figure 7B), demonstrating the importance of maintaining proper levels of
405 MurD. Having identified MurD as a key player in the regulation of cell size, we reconsidered the
406 growth media type and analyzed whether increasing *murD* expression alone results in cell size
407 changes when cells are grown in rich media. Indeed, our data revealed that induction of *murD* in
408 the merodiploid strain with native levels of DnaA grown in rich media displayed a ~10% reduction
409 in cell length compared to empty vector control without impacting growth rate. (Figure 7C,D).
410 These findings support MurD's involvement in cell size regulation that is independent of growth
411 media type.

412

413 *MurD's impact on cell size is conserved*

414 The gene encoding *murD* is part of the division and cell wall (dcw) gene cluster that is highly
415 conserved across bacteria in both order of genes and content of genes (Megrian et al., 2022;
416 Nikolaichik & Donachie, 2000). Having identified MurD as a key player of cell size, we posit
417 whether MurD's impact on cell size was conserved outside the alpha-proteobacterium *C.*
418 *crescentus*. To address this question, we used the evolutionarily distant gamma-proteobacterium
419 *Escherichia coli*. We constructed a *murD* merodiploid *E. coli* strain with the second copy of *murD*
420 expressed from the arabinose-inducible low copy expression vector *pBAD* (MG1565 p(*murD*)).
421 *E. coli* cells were induced for 3 h and analyzed at OD_{600nm} between 0.2 – 0.3. Notably, our data
422 revealed that *E. coli* with *murD* overexpression displayed ~10% reduction in cell size compared
423 to the empty vector control (Figure 7E). This change in cell size did not impact the doubling rate
424 of cells (Figure 7F). These data suggest that the role of MurD in modulating cell size is conserved
425 among bacteria.

426 **DISCUSSION**

427 Despite significant advances in our understanding of how environmental and genetic
428 perturbations can impact cell size within a population, details about the molecular mechanisms
429 underlying bacterial cell size regulation have remained elusive. One emerging insight is that the
430 regulation of cell size is governed by a complex and multifactorial process. In this study, we
431 examined the influence of the replication initiator DnaA with cell size independent of *oriC* copy
432 numbers. Our data revealed that DnaA is involved in cell size regulation through DnaA's activity
433 as a transcription factor. By inducing a modest increase (3-fold) in DnaA levels without altering
434 initiation or progression of chromosome replication, our data revealed that cells reduce their
435 elongation rate resulting in cells with smaller cell length. We show that DnaA impacts cell size by
436 indirectly regulating the transcriptional levels of key enzymes involved in cell wall biosynthesis.

437 DnaA is a global transcriptional regulator in bacteria. DnaA's transcriptional regulon commonly
438 includes other global regulators involved in genome maintenance, cell development, and
439 pathogenesis (Krusenstjerna et al., 2023). In *B. subtilis*, DnaA is connected to the onset of
440 sporulation by transcriptionally regulating an inhibitor of the sporulation master transcription factor
441 SpoOA. In *Borrelia burgdorferi*, DnaA regulates the transcription of the nucleoid associated
442 protein EbfC which itself regulates the transcription of a multitude of other genes (Jutras et al.,
443 2012; Krusenstjerna et al., 2023). Furthermore, altering the transcriptional activity of DnaA in *B.*
444 *burgdorferi* lead to changes in >20 components of the elongasome and divisome, which could
445 also connect DnaA to cell wall biosynthesis (Krusenstjerna et al., 2024). Our work revealed that
446 in *C. crescentus*, DnaA regulates cell size by modulating cell wall biosynthesis through the
447 activation of its master transcription factor GcrA. These findings highlight the global impact of
448 DnaA and its conserved ability to coordinate cell development in bacteria directly and indirectly.

449 Another major cell cycle regulator implicated in the regulation of cell size is the tubulin-like FtsZ
450 protein. The activity of FtsZ (GTP-dependent polymerization) is regulated by multiple factors that
451 promote the assembly or disassemble of the polymer. The levels of FtsZ are regulated at the
452 transcriptional level and by ATP-dependent proteolysis (Morrison & Camberg, 2024; Weart &
453 Levin, 2003). In *C. crescentus*, the expression of *ftsZ* and proteolysis of FtsZ are tightly regulated
454 over the cell cycle (Iniesta et al., 2006; Kelly et al., 1998; J. M. Schrader et al., 2016; Williams et
455 al., 2014). The accumulation of threshold levels of FtsZ were shown to be critical for determining
456 cell size in both *E. coli* and *B. subtilis* (Si et al., 2019). An increase in *ftsZ* transcription in our 3x-
457 DnaA small cells initially suggested an earlier onset and/or faster constriction rate that would lead
458 to smaller cells. Despite the 3-fold increase in transcript of *ftsZ*, the 3x-DnaA small cells displayed
459 the same concentrations of FtsZ protein as wildtype cells and thus exhibited no changes during
460 constriction. Unlike FtsZ, our increase in transcription of *dnaA* led to a corresponding increase in
461 the levels of the protein DnaA: ~3-fold increase in *dnaA* transcript led to ~3-fold increase in DnaA

462 protein levels. These findings highlight the distinctions in the multi-tiered regulation of two principal
463 cell cycle regulators, DnaA and FtsZ, both of which influence cell size.

464 Cell wall biosynthesis has been implicated with cell size regulation in bacteria (Cesar &
465 Huang, 2017). *B. subtilis* regulates cell width by balancing the activity of two opposing
466 mechanisms involved in cell wall remodeling: Rod complex and class A penicillin-binding proteins
467 (aPBPs) (Dion et al., 2019). In *C. crescentus*, deregulation of the inhibitor AimB of the cytoskeletal
468 protein MreB (part of the Rod complex) was shown to impact cell shape and cell length (Werner
469 et al., 2020). Our data revealed that small cells with 3-fold higher levels of DnaA upregulate the
470 expression of the transcription factor GcrA and the expression of cell wall biosynthetic enzymes
471 MurD and MraY. GcrA regulates the transcription of the operon where *murD* and *mraY* are found
472 side-by-side. The organization of *murD*, *mraY* and other essential genes involved in cell wall
473 biosynthesis is remarkably conserved in bacterial (Megrian et al., 2022). Increasing the
474 expression of *gcrA* or *mraY* both led to cells with increased cell length. However, increasing the
475 expression of *murD* alone led to a reduction in cell length without altering the growth rate of those
476 cells. These data indicate that DnaA regulates the levels of various factors involved in cell wall
477 biosynthesis and cell cycle progression, which collectively function to control cell size.

478 Bacteria have been known to follow the Growth law, which states that cell size is an
479 exponential function of growth rate (Donachie et al., 1976; Sargent, 1975; M. Schaechter et al.,
480 1958; Weart et al., 2007; Woldringh et al., 1980). We show that MurD's impact on cell size is
481 independent of nutrient availability. Cells with increased *murD* expression in wildtype background
482 reduced their size when grown in minimal or rich media. We discovered that further increase of
483 *murD* expression results in a further reduction in cell size that was interestingly accompanied by
484 a decrease in growth rate. This phenomenon may be attributed to the reduced cellular volume
485 interfering with essential housekeeping processes during the cell cycle or a potential connection
486 between MurD and the Growth Law. Our finding that MurD can also reduce the size in *E. coli* posit
487 MurD as a conserved regulator of cell size. MurD has garnered significant attention in drug
488 development due to its crucial role in cell wall biosynthesis (Azam & Jupudi, 2020; Sink et al.,
489 2013). This interest is likely to further escalate if MurD is found also critical for regulating cell size.
490 Further investigation into MurD's activity and its role in cell size regulation will yield significant
491 insights into the complex mechanisms governing bacterial cell size.

492 **RESOURCE AVAILABILITY**

493 All data are contained within the manuscript.

494 **ACKNOWLEDGEMENTS**

495 We are grateful to Erin Goley and her lab for providing the FtsZ antibodies, specifically to Jordan
496 M. Barrows for his assistance with the rate of elongation and constriction protocol. We thank
497 Anuradha Sharma from the Sanfilippo lab for her help with the R script. We also thank Dr. Alvaro
498 Hernandez and the Roy J. Carver Biotechnology Center for RNA sequencing, as well as to Dr.
499 Jenny Drnevich for her expertise in the statistical analysis of the RNA-seq data. The work reported
500 in this publication was supported by the National Institute of General Medical Sciences of the
501 National Institutes of Health (NIH) under Award Number R01GM133833 and by the National
502 Science Foundation (NSF) Science and Technology Center for Quantitative Cell Biology under
503 Award Number 2243257.

504 **AUTHOR CONTRIBUTIONS**

505 EK and PEM conceived project and wrote manuscript. EK performed all experiments.

506 **DECLARATION OF INTERESTS**

507 The authors declare no completing interests.

508 **FIGURE LEGENDS**

509 **Figure 1. DnaA levels impact cell size. A.** (Left) Schematic representation of *Caulobacter*
510 dimorphic lifestyle, highlighting swarmer and stalk cell. **B**. Schematic of WT and *dnaA* inducible
511 strain. Representative images of mixed population WT (CB15N *parB*::CFP-*parB*) and inducible
512 *dnaA* (CB15N Δ*vanA parB*::CFP-*parB vanA*::*dnaA dnaA*::Ω-(spec/strp) cells grown in minimal
513 media, scale 2μm. Cells were grown overnight with PYE or M2G to exponential phase with
514 relevant inducer before microscopy. **C.** Super plots showing cell length analysis of mixed
515 population grown in rich media (PYE) and minimal media (M2G). Small dots represent data points
516 from three independent replicates, large dots represents median values (blue, pink, yellow). The
517 horizontal line represents the mean of three median values. *dnaA* inducible shows ~20% decrease
518 in cell size when grown in minimal media. **D.** Super plots showing cell width analysis of mixed
519 population grown in rich media (PYE) and minimal media (M2G). **E**. Percentage cells representing
520 *oriC* quantification in WT and inducible *dnaA* strain **F.** Growth curves (top panel) representing rich
521 media and lower panel representing minimal media. WT is shown as blue dots and *dnaA* inducible
522 as yellow dots. **G.** Super plots showing cell length analysis of synchronized population grown in
523 rich media (PYE) and minimal media (M2G). Data points show mean ± SD. A parametric t test
524 was performed using population mean values (N = 3) to compare values for each measurement.
525 p(<0.0001) ****, p(0.0001)***, p(<0.05)*, ns (non-significant). n= ~600 cells

526 **Figure 2. Changing DnaA levels corelates to cell size.** Cells were grown overnight in M2G or
527 PYE to exponential phase with inducer before sample preparation and microscopy. **A.** Western
528 blot showing DnaA levels of WT and inducible *dnaA* (CB15N Δ*vanA parB*::CFP-*parB* vanA::*dnaA*
529 *dnaA*::Ω-(spec/strp) cells grown in rich and minimal media. Quantification of western blot showing
530 significant differences in *dnaA* inducible vs WT grown in minimal media. Inducible *dnaA* strain
531 shows 3-fold more DnaA in comparison to WT. **B.** Western Blot showing DnaA titration using WT
532 and inducible *dnaA* (CB15N Δ*vanA parB*::CFP-*parB xylX*::*dnaA dnaA*::Ω-(spec/strp). Levels of
533 DnaA were titrated using inducible *dnaA* strain using xylose as inducer. Xylose was titrated from
534 0.025%, 0.05%, 0.075% to 0.3% in M2G, cells grown in M2X are shown after the dotted line. **C.**
535 Quantification of DnaA levels show as the inducer percentage increases, DnaA levels are
536 increased in the inducible strain in comparison to WT in minimal media. **D.** Super plots showing
537 cell length analysis of mixed population grown in minimal media. WT (CB15N *parB*::CFP-*parB*)
538 and titration of inducer with inducible *dnaA* (CB15N Δ*vanA parB*::CFP-*parB xylX*::*dnaA dnaA*::Ω-
539 (spec/strp) strain. Small dots represent data points from three independent replicates, large dots
540 represent median values (blue,grey,orange). At 0.025% xylose the cell size reverts to WT. As the
541 concentration of inducer is increased to 0.050, 0.075, 0.03% in minimal media M2G the cell size
542 decreases gradually, whereas M2X shows further decrease in cell length ~20%. **E.** Quantification
543 of cell length in comparison to WT, the maximum drop is observed with M2X. Data points show
544 mean ± SD. A parametric t test was performed using population mean values (N = 3). p(<0.0001)
545 ****, p(0.0001)***, p(<0.05)*, ns (non-significant). n= ~600 cells
546
547 **Figure 3. Impact of DnaA on cell size determinants.** To test rate of elongation and contriction
548 cells were grown in minimal media overnight with inducer 100μM van to exponential phase before
549 synchrony, timelapse images were taken after very 15minutes. **A.** Representative time-lapse
550 images of WT (CB15N *parB*::CFP-*parB*) and 3x-DnaA (CB15N Δ*vanA parB*::CFP-*parB*
551 *vanA*::*dnaA dnaA*::Ω-(spec/strp) one cell cycle in minimal media, scale 2μm. Both WT and 3x-
552 DnaA constricts at the same time ~105-120 minutes. **B.** Quantification of rate of constriction
553 remains unchanged between WT and 3x-DnaA. **C.** Quantification of rate of elongation shows it is
554 reduced by ~20% in 3x-DnaA cells. Data points show mean ± SD. A parametric t test was
555 performed using population mean values (N = 3). n=~300 cells. **D.** Impact of protein synthesis
556 inhibition on cell size. *Caulobacter* cells were grown in minimal media overnight with sub-lethal
557 concentration of Chloramphenicol and inducer 100μM van. Super plots showing cell length
558 analysis of mixed population. Small dots represent data points from three independent replicates,
559 large dots represent median values (blue,pink,yellow). WT (CB15N *parB*::CFP-*parB)* cells show
560 a reduction in cell length by approximately 10%, while cell width remained unchanged. 3x-DnaA
561 (CB15N Δ*vanA parB*::CFP-*parB vanA*::*dnaA dnaA*::Ω-(spec/strp) cells show a further
562 approximately 10 % reduction when exposed to chloramphenicol. **E.** Impact of ppGpp on cell size.
563 Super plots showing cell length analysis of mixed population grown in minimal media. WT delta
564 *spoT (*CB15N *parB*::CFP-*parB* Δ*spoT* Δ*vanA)* in comparison to 3x-DnaA delta *spoT* (CB15N
565 Δ*vanA parB*::CFP-*parB vanA*::*dnaA dnaA*::Ω-(spec/strp Δ*spoT*). Cell length analysis shows non-

significant changes between 3x-DnaA and 3x-DnaA delta *spoT*, shows similar decrease in cell length ~20%. Data points show mean ± SD. A parametric t test was performed using population mean values (N = 3). p(<0.0001) ****, p(0.0001)***, p(<0.05)*, ns (non-significant). n= ~600 cells.

Figure 4. DnaA's ability to bind to ATP and DNA is required to cell size regulation

A. AlphaFold model of DnaA, domains color coded in blue- domain I, grey- domain II, yellow- domain III, red- domain IV. DnaA truncations show WT and mutant DnaA. Schematic shows WT and 3x-DnaA (merodiploid WT *dnaA* under P_{xyl}) (CB15N *parB*::CFP-*parB,* P_{xyl}-*dnaA)*. Cells were grown overnight in minimal media M2G or M2X (xylose as inducer) to exponential phase before serial dilution**,** western sample preparation and microscopy. **B.** Colony forming units showing viability of DnaA mutants in comparison to empty vector EV (CB15N *parB*::CFP-*parB* pXCHYC-2). EV and DnaA mutants show similar growth. **C.** Western blot showing levels of DnaA mutants in comparison to EV and 3x-DnaA. Truncation of domain IV yields 38kDa DnaA. **D.** Superplots showing cell length quantification of EV and DnaA mutants. Small dots represent data points from three independent replicates, large dots represent median values. 3x-DnaA shows ~20% decrease in cell length. Δ*ala* rich region from N-terminus (CB15N *parB*::CFP-*parB* P_{xyl}-Δ*ala* N-ter *dnaA*) shows ~15% decrease in cell length. DnaA ATP*K195I (CB15N *parB*::CFP-*parB* P_{xyl}-*dnaA* ^{K195I}*)* and DnaA domain IV truncation (CB15N *parB*::CFP-*parB* P_{xyl}-*dnaA* ^{I,II,III}) reverts back to WT cell length ~2.36μm. Data points show mean ± SD. A parametric t test was performed using population mean values (N = 3). p(<0.0001) ****, p(0.0001)***, p(<0.05)*, ns (non-significant). n=~600 cells

Figure 5. Replication progression remains unchanged in small cells. Cells were grown in minimal media M2G or M2X (xylose as inducer) with 100μM van overnight to exponential phase before synchrony. Timelapse images were taken after very 5minutes for DnaN, and every 15min for *parS* and PleC. **A.** Assembly of replisome using fluorescently tagged DnaN in WT (CB15N *parB*::CFP-*parB dnaN*::*dnaN* mcherry) and 3x-DnaA (CB15N Δ*vanA parB*::CFP-*parB vanA*::*dnaA dnaA*::Ω-(spec/strp) *dnaN*::*dnaN* mcherry). In both strains replisome assembles at ~5min represented with red dot. **B.** Timing of replication initiation was quantified using labelled ParB in WT (CB15N *parB*::CFP-*parB*) and 3x-DnaA (CB15N Δ*vanA parB*::CFP-*parB vanA*::*dnaA dnaA*::Ω-(spec/strp). In both strains, replication initiation happens at ~15-20min, represented with green dot. **C.** Progression of replication using *parS*(pMT1) near the *pleC* locus in WT (CB15N CFP-*parB PvanA*-mCherry-*parB*(pMT1) *parS*(pMT1)-*pleC* (MS513) and 3x-DnaA (CB15N CFP-*parB PvanA*-mCherry-*parB*(pMT1) *parS*(pMT1)-*Pxyl-dnaA*). In both strains we see a second PleC tag appears around ~75min, represented as red dot. Data is representation of three independent experiments. Data points show mean ± SD. A parametric t test was performed using population mean. p(<0.0001) ****, p(0.0001)***, p(<0.05)*, ns (non-significant). n=~100 cells.

603 **Figure 6. DnaA regulates cell size as a transcription factor.** Cells were grown in minimal media
604 M2G or M2X (xylose as inducer) overnight to exponential phase before RNA extraction, sample
605 preparation and microscopy. **A.** RNA-seq data represented as volcano plot (left panel) comparing
606 EV (CB15N *parB*::CFP-*parB* pXCHYC-2 to 3x-DnaA (CB15N *parB*::CFP-*parB* P_{xyl}-*dnaA*)
607 represented with dark grey shows 48 genes upregulated and 10 genes downregulated FDR <0.05.
608 Comparison of 3x-DnaA to DnaA K195I (CB15N *parB*::CFP-*parB* P_{xyl}-*dnaA* ^{K195I} is represented
609 with blue dots. **B.** FtsZ levels in WT and 3x-DnaA strain shows comparable levels, FtsZ ~65kDa.
610 **C.** Cell images of EV and merodiploid *ftsZ*, *gcrA*, *dnaG*, *mraY* and *murD,* scale 2µm. Super plots
611 showing cell length quantification of EV (CB15N *parB*::CFP-*parB* pXCHYC-2) and merodiploid
612 (CB15N *parB*::CFP-*parB* P_{xyl}-*ftsZ),* (CB15N *parB*::CFP-*parB* P_{xyl}-*gcrA),* (CB15N *parB*::CFP-*parB*
613 P_{xyl}-*dnaG),* (CB15N *parB*::CFP-*parB* P_{xyl}-*mraY),* (CB15N *parB*::CFP-*parB* P_{xyl}-*murD).* Small dots
614 represent data points from three independent replicates, large dots represent median values
615 Induction of *murD* shows 10% decrease in cell length in comparison to EV in minimal media.
616
617 **Figure 7. MurD's impact on cell size.** *Caulobacter* cells were grown in minimal media M2G or
618 M2X (xylose as inducer) with 100µM van overnight to exponential phase before microscopy. **A.**
619 Super plots showing cell length quantification of *murD* overexpression. Small dots represent data
620 points from three independent replicates, large dots represent median values. *murD*
621 overexpression in 3x-DnaA background (CB15N Δ*vanA parB*::CFP-*parB vanA*::*dnaA dnaA*::Ω-
622 (spec/strp, P_{xyl}-*murD*) results in an additional ~10% decrease in cell length in comparison to 3x-
623 DnaA (CB15N Δ*vanA parB*::CFP-*parB vanA*::*dnaA dnaA*::Ω-(spec/strp).
624 **B.** Growth curves showing induction of *murD* in 3x-DnaA cells leads to a defect on growth rate.
625 **C.** Super plots showing cell length quantification *murD* merodiploid (CB15N *parB*::CFP-*parB* P_{xyl}-
626 *murD)* in rich media (PYE) or (PYEX) xylose 0.2% was used to induce expression. *murD*
627 overexpression in rich media shows a similar 10% decrease in cell length. N=~600 cells **D.** Growth
628 curves showing the doubling time remains same when *murD* is overexpressed.
629 *E. coli* cells were grown overnight in LB and then back diluted in fresh media with 2% arabinose
630 to induce the expression for 3hrs. Cultures in early exponential phase were used for microscopy
631 and growth curves. **E.** *E. coli* cells grown in rich media. EV (MG1655-pBad) is shown in
632 comparison to *murD* overexpression (MG1565 pBad-*murD*) in rich media with and without inducer
633 arabinose 2%. Cell length decreases by ~10% when *murD* is expressed in comparison to EV with
634 inducer. **F.** Growth curves show that there is no growth defect when *murD* is overexpressed in
635 comparison to EV with and without inducer. Data points show mean ± SD. A parametric t test was
636 performed using population mean values (N = 3). p(<0.0001) ****, p(0.0001)***, p(<0.05)*, ns
637 (non-significant).
638 N=~250 cells
639

640 **MATERIALS AND METHODS**

641

642 **Bacterial strains and growth conditions**

643 Plasmids, strains, and primer descriptions are listed in the Supplementary Table S2. *Caulobacter*
644 *crescentus* strains used in this study were derived from NA1000 (wildtype). Plasmids were
645 constructed by cloning PCR products into pNPTS138,pXCHYC-2, pXMCS-2, pBXMCS-2, pBad
646 vectors (Thanbichler et al., 2007). Amplified PCR products were placed in vectors via Gibson or
647 restriction cloning. Plasmids were transformed into DH5α cells and verified through sequencing.
648 In *C. crescentus*, plasmids were transformed via electroporation. *Caulobacter* strains were grown
649 in peptone yeast extract (PYE) or M2 minimal media supplemented with 0.2% glucose (M2G) or
650 0.2% xylose (M2X). Liquid cultures were re-inoculated overnight in fresh media to grow cells until
651 exponential phase OD_{600} ~ 0.3-0.4 at 30°C under mechanical agitation 200 rpm. Overnight
652 cultures were supplemented with specific antibiotics and inducers. Vanillate 100μM was used to
653 induce the expression of $P_{van,}$ while 0.3% xylose or M2X was used to induce P_{xyl}. Liquid cultures
654 were supplemented with following concentrations of antibiotics: 5µg/ml kanamycin, 25µg/ml
655 spectinomycin, 5µg/ml streptomycin. For PYE plates 25µg/ml kanamycin, 100µg/ml
656 spectinomycin and 5µg/ml streptomycin. To check the impact of chloramphenicol, cerulenin and
657 fosfomycin, 1/10 sub-lethal concentration of chloramphenicol, 0.6µg/ml cerulenin and 5µg/ml
658 fosfomycin was added to liquid culture and left overnight such that the OD is 0.3 next day.
659 *E. coli* strains were inoculated from freezer stock grown in LB at 37°C, liquid culture was
660 supplemented with 50µg/ml ampicillin. Cultures were back diluted with antibiotic and inducer
661 arabinose 2% until exponential phase OD_{600} ~ 0.2-0.3.

662

663 **Synchronization**

664 *C.crescentus* cells were synchronized using mini-synchrony protocol to isolate swarmer
665 population (Tsai & Alley, 2001). Cells were inoculated in 15ml M2G overnight, to an OD_{600} ~ 0.3.
666 Cultures were supplemented with inducer and antibiotics as noted. Cells were pelleted at 6000
667 rpm for 10 minutes at 4°C in centrifuge. Cell pellet was resuspended in 800µl of 1X M2 salts and
668 900µl of Percoll (Sigma-Aldrich) for density gradient. The mixed solution was centrifuged at
669 11.000rpm for 20minutes, the bottom layer of swarmer cells was isolated and transferred to a
670 fresh tube. Cells were washed twice with ice cold 1X M2 salts, centrifuged at 8000 rpm for 3
671 minutes at 4°C. Swarmer's were resuspended in M2G to appropriate OD_{600} ~0.2-0.3.

672

673 **Growth assays**

674 *C.cresentus* overnight cultures were grown from freezer stock in M2G or PYE liquid medium were
675 back diluted to reach OD_{600} ~0.1 for growth curves. Early log phase cultures were used for
676 inoculation in 96-well plate in M2G or PYE with relevant inducer. Optical density at 600 nm was
677 monitored every hour at 30°C in a Biotek EPOCH-2 microplate reader with shaking. For *E. coli*,
678 cultures were inoculated from freezer stock and back diluted such that the cells reach early log

679 phase OD_{600} ~0.1 to inoculate in LB in 96-well plate. Optical density at 600 nm was monitored
680 every 10 minutes at 37°C in a Biotek EPOCH-2 microplate reader with shaking.
681
682 **Microscopy**
683 Cells were grown to an exponential OD_{600} ~0.3. Cells (1µl) were spotted on agar pads (1%
684 agarose in M2G or M2salts). For time-lapses (2µl) cells were spotted on agar pads.
685 Phase contrast and fluorescent images were taken at room temperature using Zeiss Axio
686 Observer 2.1 inverted microscope with AxioCam 506 mono camera (objective: Plan-apochromat
687 100x/1.40 Oil Ph3 M27 [WD=0.17mm]) and Zen Pro software. Samples were blinded for data
688 analysis. To count number of foci, ImageJ (cell counter plugin) was used (Schindelin, Arganda-
689 Carreras, Frise, Kaynig, Longair, Pietzsch, Preibisch, Rueden, Saalfeld, & Schmid, 2012). Cell
690 size (length and width) was analyzed using ImageJ/FIJI plugin MicrobeJ (Ducret et al., 2016).
691 Multiple frames were analyzed for cell size analysis, data were presented in Superplots (Lord et
692 al., 2020).
693
694 **Elongation and constriction**
695 Cells were grown in liquid cultures with inducer overnight to reach early log phase OD_{600} ~0.3 to
696 synchronize. After synchrony cell were resuspended in M2G or M2X with appropriate additives.
697 Cells were then spotted on agar pads (0.1% agar with inducer) for timelapse. Images were taken
698 after every 15 minutes through one cell cycle. MicrobeJ was used to analyze timelapse images
699 as described by (Lariviere et al., 2018; Mahone et al., 2024). Constriction is automatically detected
700 at the positive curvature midcell and manually segmented upon division. Cell width was detected
701 at the site of constriction whereas cell length was calculated at each time point. Cell width was
702 detected at the site of constriction whereas cell length was calculated at each time point.
703 Constriction time was determined by multiplying the number of frames from constriction initiation
704 to division by 15 (images were taken every 15min). The constriction rate was calculated by
705 dividing the cell width at the onset of constriction by the constriction time. Elongation rate
706 calculated by dividing change in length from constriction initiation to division by constriction time.
707
708 **Immunoblotting**
709 *Caulobacter* mixed population cells were grown to early exponential phase OD_{600} ~0.3 with
710 inducer. The OD_{600} of the incubated cultures was normalized to 0.2. Cells were pelted and
711 resuspended in 40µl of cracking buffer, then boiled for 10 min at 90°C. Samples were stored at -
712 20°C for western blotting. A 12% SDS-PAGE gel was used to separate proteins and then
713 transferred to PVD membrane using iBlot2 (Invitrogen Dry Blotting System). The membrane was
714 blocked with 1XTBS (10mM Tris-HCL, pH8,150mM NaCl, 0.1% Tween-20), 0.1% tween 20
715 (TBST) and 5% non-fat milk at room temperature. The blot was incubated overnight with primary
716 antibody for DnaA (α-DnaA) (Mera et al., 2014) at a dilution of 1:15,000 for FtsZ (α-
717 FtsZ)(Sundararajan et al., 2015) at a 1:20,000 dilution in TBST with 5% milk overnight at 4°C.
718 Next day the membrane was washed 3X with TBST and then incubated with secondary antibody

719 (α-Rabbit IgG peroxidase, Sigma-Aldrich) diluted to 1:15,000 in TBST with 5% milk at room
720 temperature for 1 hour. The blot was washed 3X with TBST for 5 minutes. To develop the blot,
721 SuperSignal West Pico PLUS Chemiluminescent Substrate (Themo Fisher Scientific) was used
722 and imaged by using ChemiDoc-MP (Bio-Rad). WT DnaA runs at 56kDa, whereas WT FtsZ is
723 54.1kDa, but it runs at ~65kDa.
724
725 **CFUs for viability assay**
726 *Caulobacter* cells were grown from freezer stocks in minimal media M2G or M2X, it was then
727 reinoculated in fresh media with relevant additives at 30°C 180rpm to reach exponential growth
728 OD_{600} ~0.3. Cells were then normalized to OD_{600} ~0.1. Cultures were serially diluted in a 96-well
729 plate and plated on M2G or M2X plates (0.2% xylose in M2X plates was used as inducer). Plates
730 were incubated at 30°C for 2 days and then imaged using ChemiDoc-MP (Bio-Rad).
731
732 **RNA-sequencing**
733 *Caulobacter* cells were grown from freezer stocks in minimal media M2G, reinoculated in fresh
734 media M2G or M2X (M2X media to induce the expression of mutants) at 30°C 180rpm to reach
735 exponential growth OD_{600} ~0.3. Total RNA was extracted using hot phenol procedure (Aiba et al.,
736 1981). After total RNA extraction it was treated with DNase (Invitrogen TURBO DNase) to remove
737 genomic DNA and quantitated using nanodrop (Themo Fisher Scientific NanoDrop One[c]).
738 Samples were then sent to Roy J. Carver Biotechnology Center Sequencing core at UIUC to
739 check RNA integrity through Bioanalyzer, library preparation, sequencing, and data analysis.

740 **REFERENCES**
741

742 1. Aaron, M., Charbon, G., Lam, H., Schwarz, H., Vollmer, W., & Jacobs-Wagner, C. (2007).
743 The tubulin homologue FtsZ contributes to cell elongation by guiding cell wall precursor
744 synthesis in Caulobacter crescentus. *Molecular Microbiology, 64*(4), 938-952.
745 https://doi.org/https://doi.org/10.1111/j.1365-2958.2007.05720.x
746
747 2. Aiba, H., Adhya, S., & de Crombrugghe, B. (1981). Evidence for two functional gal
748 promoters in intact Escherichia coli cells. *Journal of Biological Chemistry, 256*(22),
749 11905-11910.
750
751 3. Amir, A. (2014, 05/23/). Cell Size Regulation in Bacteria. *Physical Review Letters,*
752 *112*(20), 208102. https://doi.org/10.1103/PhysRevLett.112.208102
753
754 4. Ardissone, S., Fumeaux, C., Berge, M., Beaussart, A., Theraulaz, L., Radhakrishnan, S.
755 K., Dufrene, Y. F., & Viollier, P. H. (2014, Nov 25). Cell cycle constraints on capsulation
756 and bacteriophage susceptibility. *Elife, 3*. https://doi.org/10.7554/eLife.03587
757
758 5. Azam, M. A., & Jupudi, S. (2020, 2020/06/01). MurD inhibitors as antibacterial agents: a
759 review. *Chemical Papers, 74*(6), 1697-1708. https://doi.org/10.1007/s11696-020-01057-w
760
761 6. Banerjee, S., Lo, K., Daddysman, M. K., Selewa, A., Kuntz, T., Dinner, A. R., & Scherer,
762 N. F. (2017, Jul 24). Biphasic growth dynamics control cell division in Caulobacter
763 crescentus. *Nat Microbiol, 2*, 17116. https://doi.org/10.1038/nmicrobiol.2017.116
764
765 7. Barrows, J. M., & Goley, E. D. (2023, Feb 22). Synchronized Swarmers and Sticky
766 Stalks: Caulobacter crescentus as a Model for Bacterial Cell Biology. *J Bacteriol, 205*(2),
767 e0038422. https://doi.org/10.1128/jb.00384-22
768
769 8. Bartlett, T. M., Bratton, B. P., Duvshani, A., Miguel, A., Sheng, Y., Martin, N. R., Nguyen,
770 J. P., Persat, A., Desmarais, S. M., VanNieuwenhze, M. S., Huang, K. C., Zhu, J.,
771 Shaevitz, J. W., & Gitai, Z. (2017, Jan 12). A Periplasmic Polymer Curves Vibrio cholerae
772 and Promotes Pathogenesis. *Cell, 168*(1-2), 172-185 e115.
773 https://doi.org/10.1016/j.cell.2016.12.019
774
775 9. Basan, M., Zhu, M., Dai, X., Warren, M., Sevin, D., Wang, Y. P., & Hwa, T. (2015, Oct
776 30). Inflating bacterial cells by increased protein synthesis. *Mol Syst Biol, 11*(10), 836.
777 https://doi.org/10.15252/msb.20156178
778
779 10. Bates, D., & Kleckner, N. (2005, Jun 17). Chromosome and replisome dynamics in E.
780 coli: loss of sister cohesion triggers global chromosome movement and mediates
781 chromosome segregation. *Cell, 121*(6), 899-911.
782 https://doi.org/10.1016/j.cell.2005.04.013
783
784 11. Beveridge, T. (1988). The bacterial surface: general considerations towards design and
785 function. *Canadian Journal of Microbiology, 34*(4), 363-372.

786
787 12. Boye, E., Stokke, T., Kleckner, N., & Skarstad, K. (1996, Oct 29). Coordinating DNA
788 replication initiation with cell growth: differential roles for DnaA and SeqA proteins. *Proc*
789 *Natl Acad Sci U S A, 93*(22), 12206-12211. https://doi.org/10.1073/pnas.93.22.12206
790
791 13. Cabeen, M. T., Charbon, G., Vollmer, W., Born, P., Ausmees, N., Weibel, D. B., &
792 Jacobs-Wagner, C. (2009, May 6). Bacterial cell curvature through mechanical control of
793 cell growth. *Embo j, 28*(9), 1208-1219. https://doi.org/10.1038/emboj.2009.61
794
795 14. Campos, M., Surovtsev, I. V., Kato, S., Paintdakhi, A., Beltran, B., Ebmeier, S. E., &
796 Jacobs-Wagner, C. (2014, Dec 4). A constant size extension drives bacterial cell size
797 homeostasis. *Cell, 159*(6), 1433-1446. https://doi.org/10.1016/j.cell.2014.11.022
798
799 15. Cesar, S., & Huang, K. C. (2017, Sep 1). Thinking big: the tunability of bacterial cell size.
800 *FEMS Microbiol Rev, 41*(5), 672-678. https://doi.org/10.1093/femsre/fux026
801
802 16. Churchward, G., Estiva, E., & Bremer, H. (1981, Mar). Growth rate-dependent control of
803 chromosome replication initiation in Escherichia coli. *J Bacteriol, 145*(3), 1232-1238.
804 https://doi.org/10.1128/jb.145.3.1232-1238.1981
805
806 17. Collier, J., Murray, S. R., & Shapiro, L. (2006, 2006/01/25). DnaA couples DNA
807 replication and the expression of two cell cycle master regulators. *The EMBO Journal,*
808 *25*(2), 346-356-356. https://doi.org/https://doi.org/10.1038/sj.emboj.7600927
809
810 18. Collier, J., Murray, S. R., & Shapiro, L. (2006, Jan 25). DnaA couples DNA replication
811 and the expression of two cell cycle master regulators. *EMBO J, 25*(2), 346-356.
812 https://doi.org/10.1038/sj.emboj.7600927
813
814 19. Collier, J., & Shapiro, L. (2009, Sep). Feedback control of DnaA-mediated replication
815 initiation by replisome-associated HdaA protein in Caulobacter. *J Bacteriol, 191*(18),
816 5706-5716. https://doi.org/10.1128/JB.00525-09
817
818 20. Cooper, S., & Helmstetter, C. E. (1968, Feb 14). Chromosome replication and the
819 division cycle of Escherichia coli B/r. *J Mol Biol, 31*(3), 519-540.
820 https://doi.org/10.1016/0022-2836(68)90425-7
821
822 21. Cronan, J. E. (2014). A new pathway of exogenous fatty acid incorporation proceeds by a
823 classical phosphoryl transfer reaction. *Molecular microbiology, 92*(2), 217-221.
824
825 22. Dalia, A. B., & Weiser, J. N. (2011, Nov 17). Minimization of bacterial size allows for
826 complement evasion and is overcome by the agglutinating effect of antibody. *Cell Host*
827 *Microbe, 10*(5), 486-496. https://doi.org/10.1016/j.chom.2011.09.009
828
829 23. Dion, M. F., Kapoor, M., Sun, Y., Wilson, S., Ryan, J., Vigouroux, A., van Teeffelen, S.,
830 Oldenbourg, R., & Garner, E. C. (2019, Aug). Bacillus subtilis cell diameter is determined

by the opposing actions of two distinct cell wall synthetic systems. *Nat Microbiol, 4*(8), 1294-1305. https://doi.org/10.1038/s41564-019-0439-0

24. Donachie, W. D. (1968, Sep 7). Relationship between cell size and time of initiation of DNA replication. *Nature, 219*(5158), 1077-1079. https://doi.org/10.1038/2191077a0

25. Donachie, W. D., Begg, K. J., & Vicente, M. (1976, Nov 25). Cell length, cell growth and cell division. *Nature, 264*(5584), 328-333. https://doi.org/10.1038/264328a0

26. Ducret, A., Quardokus, E. M., & Brun, Y. V. (2016, Jun 20). MicrobeJ, a tool for high throughput bacterial cell detection and quantitative analysis. *Nat Microbiol, 1*(7), 16077. https://doi.org/10.1038/nmicrobiol.2016.77

27. Duderstadt, K. E., & Berger, J. M. (2013, Feb). A structural framework for replication origin opening by AAA+ initiation factors. *Curr Opin Struct Biol, 23*(1), 144-153. https://doi.org/10.1016/j.sbi.2012.11.012

28. Evinger, M., & Agabian, N. (1977, Oct). Envelope-associated nucleoid from Caulobacter crescentus stalked and swarmer cells. *J Bacteriol, 132*(1), 294-301. https://doi.org/10.1128/jb.132.1.294-301.1977

29. Felletti, M., Omnus, D. J., & Jonas, K. (2019, Jul). Regulation of the replication initiator DnaA in Caulobacter crescentus. *Biochim Biophys Acta Gene Regul Mech, 1862*(7), 697-705. https://doi.org/10.1016/j.bbagrm.2018.01.004

30. Felletti, M., Romilly, C., Wagner, E. G. H., & Jonas, K. (2021, Sep 15). A nascent polypeptide sequence modulates DnaA translation elongation in response to nutrient availability. *Elife, 10*. https://doi.org/10.7554/eLife.71611

31. Fernandez-Fernandez, C., Gonzalez, D., & Collier, J. (2011). Regulation of the Activity of the Dual-Function DnaA Protein in Caulobacter crescentus. *PLOS ONE, 6*(10), e26028. https://doi.org/10.1371/journal.pone.0026028

32. Frandi, A., & Collier, J. (2019). Multilayered control of chromosome replication in Caulobacter crescentus. *Biochemical Society Transactions, 47*(1), 187-196. https://doi.org/10.1042/bst20180460

33. Fujikawa, N., Kurumizaka, H., Nureki, O., Terada, T., Shirouzu, M., Katayama, T., & Yokoyama, S. (2003, Apr 15). Structural basis of replication origin recognition by the DnaA protein. *Nucleic Acids Res, 31*(8), 2077-2086. https://doi.org/10.1093/nar/gkg309

34. Glenn, S., Fragasso, A., Lin, W.-H., Papagiannakis, A., Kato, S., & Jacobs-Wagner, C. (2024). Coupling of cell growth modulation to asymmetric division and cell cycle regulation in Caulobacter crescentus. *Proceedings of the National Academy of Sciences, 121*(41), e2406397121. https://doi.org/doi:10.1073/pnas.2406397121

35. Glenn, S., Fragasso, A., Lin, W. H., Papagiannakis, A., Kato, S., & Jacobs-Wagner, C. (2024, Oct 8). Coupling of cell growth modulation to asymmetric division and cell cycle regulation in Caulobacter crescentus. *Proc Natl Acad Sci U S A, 121*(41), e2406397121. https://doi.org/10.1073/pnas.2406397121

36. Goley, E. D., Dye, N. A., Werner, J. N., Gitai, Z., & Shapiro, L. (2010, 2010/09/24/). Imaging-Based Identification of a Critical Regulator of FtsZ Protofilament Curvature in Caulobacter. *Molecular Cell, 39*(6), 975-987. https://doi.org/https://doi.org/10.1016/j.molcel.2010.08.027

37. Gonzalez, D., & Collier, J. (2014, Jul). Effects of (p)ppGpp on the progression of the cell cycle of Caulobacter crescentus. *J Bacteriol, 196*(14), 2514-2525. https://doi.org/10.1128/JB.01575-14

38. Govers, S. K., & Jacobs-Wagner, C. (2020, Oct 5). Caulobacter crescentus: model system extraordinaire. *Curr Biol, 30*(19), R1151-R1158. https://doi.org/10.1016/j.cub.2020.07.033

39. Grant, N. A., Abdel Magid, A., Franklin, J., Dufour, Y., & Lenski, R. E. (2021, Apr 21). Changes in Cell Size and Shape during 50,000 Generations of Experimental Evolution with Escherichia coli. *J Bacteriol, 203*(10). https://doi.org/10.1128/JB.00469-20

40. Haakonsen, D. L., Yuan, A. H., & Laub, M. T. (2015, Nov 1). The bacterial cell cycle regulator GcrA is a sigma70 cofactor that drives gene expression from a subset of methylated promoters. *Genes Dev, 29*(21), 2272-2286. https://doi.org/10.1101/gad.270660.115

41. Hallgren, J., & Jonas, K. (2024, Feb). Nutritional control of bacterial DNA replication. *Curr Opin Microbiol, 77*, 102403. https://doi.org/10.1016/j.mib.2023.102403

42. Hansen, F. G., & Atlung, T. (2018). The DnaA Tale. *Front Microbiol, 9*, 319. https://doi.org/10.3389/fmicb.2018.00319

43. Hansen, F. G., Hansen, E. B., & Atlung, T. (1982). The nucleotide sequence of the dnaA gene promoter and of the adjacent rpmH gene, coding for the ribosomal protein L34, of Escherichia coli. *EMBO J, 1*(9), 1043-1048. https://doi.org/10.1002/j.1460-2075.1982.tb01294.x

44. Harris, L. K., & Theriot, J. A. (2016, Jun 2). Relative Rates of Surface and Volume Synthesis Set Bacterial Cell Size. *Cell, 165*(6), 1479-1492. https://doi.org/10.1016/j.cell.2016.05.045

45. Helmstetter, C., Cooper, S., Pierucci, O., & Revelas, E. (1968). On the bacterial life sequence. *Cold Spring Harb Symp Quant Biol, 33*, 809-822. https://doi.org/10.1101/sqb.1968.033.01.093

46. Hill, N. S., Kadoya, R., Chattoraj, D. K., & Levin, P. A. (2012). Cell size and the initiation of DNA replication in bacteria. *PLoS Genet, 8*(3), e1002549. https://doi.org/10.1371/journal.pgen.1002549

47. Ho, P.-Y., & Amir, A. (2015). Simultaneous regulation of cell size and chromosome replication in bacteria. *Frontiers in microbiology, 6*, 662.

48. Holtzendorff, J., Hung, D., Brende, P., Reisenauer, A., Viollier, P. H., McAdams, H. H., & Shapiro, L. (2004, May 14). Oscillating global regulators control the genetic circuit driving a bacterial cell cycle. *Science, 304*(5673), 983-987. https://doi.org/10.1126/science.1095191

49. Hottes, A. K., Shapiro, L., & McAdams, H. H. (2005). DnaA coordinates replication initiation and cell cycle transcription in Caulobacter crescentus. *Molecular Microbiology, 58*(5), 1340-1353. https://doi.org/https://doi.org/10.1111/j.1365-2958.2005.04912.x

50. Hottes, A. K., Shapiro, L., & McAdams, H. H. (2005, Dec). DnaA coordinates replication initiation and cell cycle transcription in Caulobacter crescentus. *Mol Microbiol, 58*(5), 1340-1353. https://doi.org/10.1111/j.1365-2958.2005.04912.x

51. Ikeda, M., Wachi, M., Jung, H. K., Ishino, F., & Matsuhashi, M. (1991, Feb). The Escherichia coli mraY gene encoding UDP-N-acetylmuramoyl-pentapeptide: undecaprenyl-phosphate phospho-N-acetylmuramoyl-pentapeptide transferase. *J Bacteriol, 173*(3), 1021-1026. https://doi.org/10.1128/jb.173.3.1021-1026.1991

52. Iniesta, A. A., McGrath, P. T., Reisenauer, A., McAdams, H. H., & Shapiro, L. (2006, Jul 18). A phospho-signaling pathway controls the localization and activity of a protease complex critical for bacterial cell cycle progression. *Proc Natl Acad Sci U S A, 103*(29), 10935-10940. https://doi.org/10.1073/pnas.0604554103

53. Irnov, I., Wang, Z., Jannetty, N. D., Bustamante, J. A., Rhee, K. Y., & Jacobs-Wagner, C. (2017). Crosstalk between the tricarboxylic acid cycle and peptidoglycan synthesis in Caulobacter crescentus through the homeostatic control of α-ketoglutarate. *PLOS Genetics, 13*(8), e1006978. https://doi.org/10.1371/journal.pgen.1006978

54. Jensen, R. B., Wang, S. C., & Shapiro, L. (2001, Sep 3). A moving DNA replication factory in Caulobacter crescentus. *EMBO J, 20*(17), 4952-4963. https://doi.org/10.1093/emboj/20.17.4952

55. Jun, S., Si, F., Pugatch, R., & Scott, M. (2018, May). Fundamental principles in bacterial physiology-history, recent progress, and the future with focus on cell size control: a review. *Rep Prog Phys, 81*(5), 056601. https://doi.org/10.1088/1361-6633/aaa628

56. Jutras, B. L., Bowman, A., Brissette, C. A., Adams, C. A., Verma, A., Chenail, A. M., & Stevenson, B. (2012, Jul). EbfC (YbaB) is a new type of bacterial nucleoid-associated

968 protein and a global regulator of gene expression in the Lyme disease spirochete. *J*
969 *Bacteriol, 194*(13), 3395-3406. https://doi.org/10.1128/JB.00252-12
970
971 57. Kaneda, T. (1991). Iso-and anteiso-fatty acids in bacteria: biosynthesis, function, and
972 taxonomic significance. *Microbiological reviews, 55*(2), 288-302.
973
974 58. Katayama, T., Ozaki, S., Keyamura, K., & Fujimitsu, K. (2010). Regulation of the
975 replication cycle: conserved and diverse regulatory systems for DnaA and oriC. *Nature*
976 *Reviews Microbiology, 8*(3), 163-170.
977
978 59. Kelly, A. J., Sackett, M. J., Din, N., Quardokus, E., & Brun, Y. V. (1998, Mar 15). Cell
979 cycle-dependent transcriptional and proteolytic regulation of FtsZ in Caulobacter. *Genes*
980 *Dev, 12*(6), 880-893. https://doi.org/10.1101/gad.12.6.880
981
982 60. Kirkpatrick, C. L., & Viollier, P. H. (2012, Jan). Decoding Caulobacter development.
983 *FEMS Microbiol Rev, 36*(1), 193-205. https://doi.org/10.1111/j.1574-6976.2011.00309.x
984
985 61. Kohiyama, M. (2020, Dec). Research on DnaA in the early days. *Res Microbiol, 171*(8),
986 287-289. https://doi.org/10.1016/j.resmic.2020.11.004
987
988 62. Koppes, L. J., Meyer, M., Oonk, H. B., de Jong, M. A., & Nanninga, N. (1980, Sep).
989 Correlation between size and age at different events in the cell division cycle of
990 Escherichia coli. *J Bacteriol, 143*(3), 1241-1252. https://doi.org/10.1128/jb.143.3.1241-
991 1252.1980
992
993 63. Krusenstjerna, A. C., Jusufovic, N., Saylor, T. C., & Stevenson, B. (2024, Aug 29). DnaA
994 modulates the gene expression and morphology of the Lyme disease spirochete. *bioRxiv*.
995 https://doi.org/10.1101/2024.06.08.598065
996
997 64. Krusenstjerna, A. C., Saylor, T. C., Arnold, W. K., Tucker, J. S., & Stevenson, B. (2023,
998 Jan 26). Borrelia burgdorferi DnaA and the Nucleoid-Associated Protein EbfC Coordinate
999 Expression of the dnaX-ebfC Operon. *J Bacteriol, 205*(1), e0039622.
1000 https://doi.org/10.1128/jb.00396-22
1001
1002 65. Lambert, A., Vanhecke, A., Archetti, A., Holden, S., Schaber, F., Pincus, Z., Laub, M. T.,
1003 Goley, E., & Manley, S. (2018, 2018/06/29/). Constriction Rate Modulation Can Drive Cell
1004 Size Control and Homeostasis in C. crescentus. *iScience, 4*, 180-189.
1005 https://doi.org/https://doi.org/10.1016/j.isci.2018.05.020
1006
1007 66. Lariviere, P. J., Szwedziak, P., Mahone, C. R., Löwe, J., & Goley, E. D. (2018, Jan). FzlA,
1008 an essential regulator of FtsZ filament curvature, controls constriction rate during
1009 Caulobacter division. *Mol Microbiol, 107*(2), 180-197. https://doi.org/10.1111/mmi.13876
1010
1011 67. Lenski, R. E., & Travisano, M. (1994, Jul 19). Dynamics of adaptation and diversification:
1012 a 10,000-generation experiment with bacterial populations. *Proc Natl Acad Sci U S A,*
1013 *91*(15), 6808-6814. https://doi.org/10.1073/pnas.91.15.6808

68. Leonard, A. C., & Grimwade, J. E. (2011). Regulation of DnaA assembly and activity: taking directions from the genome. *Annual review of microbiology, 65*(1), 19-35.

69. Levine, A., Vannier, F., Dehbi, M., Henckes, G., & Seror, S. J. (1991, Jun 20). The stringent response blocks DNA replication outside the ori region in Bacillus subtilis and at the origin in Escherichia coli. *J Mol Biol, 219*(4), 605-613. https://doi.org/10.1016/0022-2836(91)90657-r

70. Lobner-Olesen, A., Skarstad, K., Hansen, F. G., von Meyenburg, K., & Boye, E. (1989, Jun 2). The DnaA protein determines the initiation mass of Escherichia coli K-12. *Cell, 57*(5), 881-889. https://doi.org/10.1016/0092-8674(89)90802-7

71. Lord, S. J., Velle, K. B., Mullins, R. D., & Fritz-Laylin, L. K. (2020). SuperPlots: Communicating reproducibility and variability in cell biology. *Journal of Cell Biology, 219*(6). https://doi.org/10.1083/jcb.202001064

72. Maciag, M., Kochanowska, M., Lyzen, R., Wegrzyn, G., & Szalewska-Palasz, A. (2010, Jan). ppGpp inhibits the activity of Escherichia coli DnaG primase. *Plasmid, 63*(1), 61-67. https://doi.org/10.1016/j.plasmid.2009.11.002

73. Mahone, C. R., Payne, I. P., Lyu, Z., McCausland, J. W., Barrows, J. M., Xiao, J., Yang, X., & Goley, E. D. (2024, Feb 5). Integration of cell wall synthesis and chromosome segregation during cell division in Caulobacter. *J Cell Biol, 223*(2). https://doi.org/10.1083/jcb.202211026

74. Marczynski, G. T. (1999, Apr). Chromosome methylation and measurement of faithful, once and only once per cell cycle chromosome replication in Caulobacter crescentus. *J Bacteriol, 181*(7), 1984-1993. https://doi.org/10.1128/JB.181.7.1984-1993.1999

75. Megrian, D., Taib, N., Jaffe, A. L., Banfield, J. F., & Gribaldo, S. (2022, Dec). Ancient origin and constrained evolution of the division and cell wall gene cluster in Bacteria. *Nat Microbiol, 7*(12), 2114-2127. https://doi.org/10.1038/s41564-022-01257-y

76. Menikpurage, I. P., Woo, K., & Mera, P. E. (2021). Transcriptional Activity of the Bacterial Replication Initiator DnaA. *Front Microbiol, 12*, 662317. https://doi.org/10.3389/fmicb.2021.662317

77. Mera, P. E., Kalogeraki, V. S., & Shapiro, L. (2014). Replication initiator DnaA binds at the Caulobacter centromere and enables chromosome segregation. *Proceedings of the National Academy of Sciences, 111*(45), 16100-16105.

78. Messer, W., & Weigel, C. (1997, Apr). DnaA initiator--also a transcription factor. *Mol Microbiol, 24*(1), 1-6. https://doi.org/10.1046/j.1365-2958.1997.3171678.x

79. Messer, W., & Weigel, C. (1997). DnaA initiator—also a transcription factor. *Molecular microbiology, 24*(1), 1-6.

80. Mizushima, T., Sasaki, S., Ohishi, H., Kobayashi, M., Katayama, T., Miki, T., Maeda, M., & Sekimizu, K. (1996, Oct 11). Molecular design of inhibitors of in vitro oriC DNA replication based on the potential to block the ATP binding of DnaA protein. *J Biol Chem, 271*(41), 25178-25183. https://doi.org/10.1074/jbc.271.41.25178

81. Mizushima, T., Takaki, T., Kubota, T., Tsuchiya, T., Miki, T., Katayama, T., & Sekimizu, K. (1998, Aug 14). Site-directed mutational analysis for the ATP binding of DnaA protein. Functions of two conserved amino acids (Lys-178 and Asp-235) located in the ATP-binding domain of DnaA protein in vitro and in vivo. *J Biol Chem, 273*(33), 20847-20851. https://doi.org/10.1074/jbc.273.33.20847

82. Morrison, J. J., & Camberg, J. L. (2024). Building the Bacterial Divisome at the Septum. *Subcell Biochem, 104*, 49-71. https://doi.org/10.1007/978-3-031-58843-3_4

83. Ng, T. W., Ojkic, N., Serbanescu, D., & Banerjee, S. (2024). Differential growth regulates asymmetric size partitioning in Caulobacter crescentus. *Life Science Alliance, 7*(8), e202402591. https://doi.org/10.26508/lsa.202402591

84. Ng, T. W., Ojkic, N., Serbanescu, D., & Banerjee, S. (2024, Aug). Differential growth regulates asymmetric size partitioning in Caulobacter crescentus. *Life Sci Alliance, 7*(8). https://doi.org/10.26508/lsa.202402591

85. Nikolaichik, Y. A., & Donachie, W. D. (2000). Conservation of gene order amongst cell wall and cell division genes in Eubacteria, and ribosomal genes in Eubacteria and Eukaryotic organelles. *Genetica, 108*(1), 1-7. https://doi.org/10.1023/a:1004077806910

86. Olliver, A., Saggioro, C., Herrick, J., & Sclavi, B. (2010, Jun). DnaA-ATP acts as a molecular switch to control levels of ribonucleotide reductase expression in Escherichia coli. *Mol Microbiol, 76*(6), 1555-1571. https://doi.org/10.1111/j.1365-2958.2010.07185.x

87. Sackett, M. J., Kelly, A. J., & Brun, Y. V. (1998, May). Ordered expression of ftsQA and ftsZ during the Caulobacter crescentus cell cycle. *Mol Microbiol, 28*(3), 421-434. https://doi.org/10.1046/j.1365-2958.1998.00753.x

88. Salama, N. R. (2020, Apr). Cell morphology as a virulence determinant: lessons from Helicobacter pylori. *Curr Opin Microbiol, 54*, 11-17. https://doi.org/10.1016/j.mib.2019.12.002

89. Sargent, M. G. (1975, Jul). Control of cell length in Bacillus subtilis. *J Bacteriol, 123*(1), 7-19. https://doi.org/10.1128/jb.123.1.7-19.1975

90. Schaechter, M., Maaloe, O., & Kjeldgaard, N. O. (1958, Dec). Dependency on medium and temperature of cell size and chemical composition during balanced grown of

Salmonella typhimurium. *J Gen Microbiol, 19*(3), 592-606. https://doi.org/10.1099/00221287-19-3-592

91. Schaechter, M., Maaløe, O., & Kjeldgaard, N. O. (1958). Dependency on medium and temperature of cell size and chemical composition during balanced growth of Salmonella typhimurium. *Microbiology, 19*(3), 592-606.

92. Schindelin, J., Arganda-Carreras, I., Frise, E., Kaynig, V., Longair, M., Pietzsch, T., Preibisch, S., Rueden, C., Saalfeld, S., & Schmid, B. (2012). Fiji: an open-source platform for biological-image analysis. *Nature Methods, 9*(7), 676-682.

93. Schindelin, J., Arganda-Carreras, I., Frise, E., Kaynig, V., Longair, M., Pietzsch, T., Preibisch, S., Rueden, C., Saalfeld, S., Schmid, B., Tinevez, J.-Y., White, D. J., Hartenstein, V., Eliceiri, K., Tomancak, P., & Cardona, A. (2012, 2012/07/01). Fiji: an open-source platform for biological-image analysis. *Nature Methods, 9*(7), 676-682. https://doi.org/10.1038/nmeth.2019

94. Schrader, J. M., Li, G.-W., Childers, W. S., Perez, A. M., Weissman, J. S., Shapiro, L., & McAdams, H. H. (2016). Dynamic translation regulation in Caulobacter cell cycle control. *Proceedings of the National Academy of Sciences, 113*(44), E6859-E6867.

95. Schrader, J. M., Li, G. W., Childers, W. S., Perez, A. M., Weissman, J. S., Shapiro, L., & McAdams, H. H. (2016, Nov 1). Dynamic translation regulation in Caulobacter cell cycle control. *Proc Natl Acad Sci U S A, 113*(44), E6859-E6867. https://doi.org/10.1073/pnas.1614795113

96. Schrader, J. M., & Shapiro, L. (2015, Apr 8). Synchronization of Caulobacter crescentus for investigation of the bacterial cell cycle. *J Vis Exp*(98). https://doi.org/10.3791/52633

97. Schwartz, M. A., & Shapiro, L. (2011). An SMC ATPase mutant disrupts chromosome segregation in Caulobacter. *Molecular microbiology, 82*(6), 1359-1374.

98. Sekimizu, K., Bramhill, D., & Kornberg, A. (1987, Jul 17). ATP activates dnaA protein in initiating replication of plasmids bearing the origin of the E. coli chromosome. *Cell, 50*(2), 259-265. https://doi.org/10.1016/0092-8674(87)90221-2

99. Si, F., Le Treut, G., Sauls, J. T., Vadia, S., Levin, P. A., & Jun, S. (2019, Jun 3). Mechanistic Origin of Cell-Size Control and Homeostasis in Bacteria. *Curr Biol, 29*(11), 1760-1770 e1767. https://doi.org/10.1016/j.cub.2019.04.062

100. Si, F., Li, D., Cox, S. E., Sauls, J. T., Azizi, O., Sou, C., Schwartz, A. B., Erickstad, M. J., Jun, Y., & Li, X. (2017). Invariance of initiation mass and predictability of cell size in Escherichia coli. *Current Biology, 27*(9), 1278-1287.

101. Si, F., Li, D., Cox, S. E., Sauls, J. T., Azizi, O., Sou, C., Schwartz, A. B., Erickstad, M. J., Jun, Y., Li, X., & Jun, S. (2017, May 8). Invariance of Initiation Mass and Predictability of

Cell Size in Escherichia coli. *Curr Biol, 27*(9), 1278-1287. https://doi.org/10.1016/j.cub.2017.03.022

102. Sink, R., Barreteau, H., Patin, D., Mengin-Lecreulx, D., Gobec, S., & Blanot, D. (2013, Dec). MurD enzymes: some recent developments. *Biomol Concepts, 4*(6), 539-556. https://doi.org/10.1515/bmc-2013-0024

103. Speck, C., Weigel, C., & Messer, W. (1999, Nov 1). ATP- and ADP-dnaA protein, a molecular switch in gene regulation. *EMBO J, 18*(21), 6169-6176. https://doi.org/10.1093/emboj/18.21.6169

104. Srivatsan, A., & Wang, J. D. (2008, Apr). Control of bacterial transcription, translation and replication by (p)ppGpp. *Curr Opin Microbiol, 11*(2), 100-105. https://doi.org/10.1016/j.mib.2008.02.001

105. Stephens, C., Christen, B., Watanabe, K., Fuchs, T., & Jenal, U. (2007). Regulation of d-Xylose Metabolism in Caulobacter crescentus by a LacI-Type Repressor. *Journal of Bacteriology, 189*(24), 8828-8834. https://doi.org/doi:10.1128/jb.01342-07

106. Stove, J. L., & Stanier, R. Y. (1962, 1962/12/01). Cellular Differentiation in Stalked Bacteria. *Nature, 196*(4860), 1189-1192. https://doi.org/10.1038/1961189a0

107. Sundararajan, K., Miguel, A., Desmarais, S. M., Meier, E. L., Casey Huang, K., & Goley, E. D. (2015, 2015/06/23). The bacterial tubulin FtsZ requires its intrinsically disordered linker to direct robust cell wall construction. *Nature Communications, 6*(1), 7281. https://doi.org/10.1038/ncomms8281

108. Taylor, J. A., Sichel, S. R., & Salama, N. R. (2019, Sep 8). Bent Bacteria: A Comparison of Cell Shape Mechanisms in Proteobacteria. *Annu Rev Microbiol, 73*, 457-480. https://doi.org/10.1146/annurev-micro-020518-115919

109. Thanbichler, M., Iniesta, A. A., & Shapiro, L. (2007). A comprehensive set of plasmids for vanillate- and xylose-inducible gene expression in Caulobacter crescentus. *Nucleic Acids Research, 35*(20), e137-e137. https://doi.org/10.1093/nar/gkm818

110. Thanbichler, M., & Shapiro, L. (2006, 08/01). MipZ, a Spatial Regulator Coordinating Chromosome Segregation with Cell Division in Caulobacter. *Cell, 126*, 147-162. https://doi.org/10.1016/j.cell.2006.05.038

111. Toro, E., Hong, S. H., McAdams, H. H., & Shapiro, L. (2008, Oct 7). Caulobacter requires a dedicated mechanism to initiate chromosome segregation. *Proc Natl Acad Sci U S A, 105*(40), 15435-15440. https://doi.org/10.1073/pnas.0807448105

112. Tozawa, Y., & Nomura, Y. (2011, Sep). Signalling by the global regulatory molecule ppGpp in bacteria and chloroplasts of land plants. *Plant Biol (Stuttg), 13*(5), 699-709. https://doi.org/10.1111/j.1438-8677.2011.00484.x

113. Traxler, M. F., Summers, S. M., Nguyen, H. T., Zacharia, V. M., Hightower, G. A., Smith, J. T., & Conway, T. (2008, Jun). The global, ppGpp-mediated stringent response to amino acid starvation in Escherichia coli. *Mol Microbiol, 68*(5), 1128-1148. https://doi.org/10.1111/j.1365-2958.2008.06229.x

114. Tsai, J.-W., & Alley, M. R. K. (2001). Proteolysis of the Caulobacter McpA Chemoreceptor Is Cell Cycle Regulated by a ClpX-Dependent Pathway. *Journal of Bacteriology, 183*, 5001 - 5007.

115. Typas, A., Banzhaf, M., Gross, C. A., & Vollmer, W. (2012, 2012/02/01). From the regulation of peptidoglycan synthesis to bacterial growth and morphology. *Nature Reviews Microbiology, 10*(2), 123-136. https://doi.org/10.1038/nrmicro2677

116. Vadia, S., Tse, J. L., Lucena, R., Yang, Z., Kellogg, D. R., Wang, J. D., & Levin, P. A. (2017, Jun 19). Fatty Acid Availability Sets Cell Envelope Capacity and Dictates Microbial Cell Size. *Curr Biol, 27*(12), 1757-1767.e1755. https://doi.org/10.1016/j.cub.2017.05.076

117. Washington, T. A., Smith, J. L., & Grossman, A. D. (2017). Genetic networks controlled by the bacterial replication initiator and transcription factor DnaA in Bacillus subtilis. *Molecular microbiology, 106*(1), 109-128.

118. Weart, R. B., Lee, A. H., Chien, A. C., Haeusser, D. P., Hill, N. S., & Levin, P. A. (2007, Jul 27). A metabolic sensor governing cell size in bacteria. *Cell, 130*(2), 335-347. https://doi.org/10.1016/j.cell.2007.05.043

119. Weart, R. B., & Levin, P. A. (2003, May). Growth rate-dependent regulation of medial FtsZ ring formation. *J Bacteriol, 185*(9), 2826-2834. https://doi.org/10.1128/JB.185.9.2826-2834.2003

120. Wells, D. H., & Long, S. R. (2002, Mar). The Sinorhizobium meliloti stringent response affects multiple aspects of symbiosis. *Mol Microbiol, 43*(5), 1115-1127. https://doi.org/10.1046/j.1365-2958.2002.02826.x

121. Werner, J. N., Shi, H., Hsin, J., Huang, K. C., Gitai, Z., & Klein, E. A. (2020, Aug 4). AimB Is a Small Protein Regulator of Cell Size and MreB Assembly. *Biophys J, 119*(3), 593-604. https://doi.org/10.1016/j.bpj.2020.04.029

122. Westfall, C. S., & Levin, P. A. (2017, Sep 8). Bacterial Cell Size: Multifactorial and Multifaceted. *Annu Rev Microbiol, 71*, 499-517. https://doi.org/10.1146/annurev-micro-090816-093803

123. Williams, B., Bhat, N., Chien, P., & Shapiro, L. (2014, Sep). ClpXP and ClpAP proteolytic activity on divisome substrates is differentially regulated following the Caulobacter asymmetric cell division. *Mol Microbiol, 93*(5), 853-866. https://doi.org/10.1111/mmi.12698

124. Willis, L., & Huang, K. (2017, 08/14). Sizing up the bacterial cell cycle. *Nature Reviews Microbiology, 15*. https://doi.org/10.1038/nrmicro.2017.79

125. Wold, S., Skarstad, K., Steen, H. B., Stokke, T., & Boye, E. (1994, May 1). The initiation mass for DNA replication in Escherichia coli K-12 is dependent on growth rate. *EMBO J, 13*(9), 2097-2102. https://doi.org/10.1002/j.1460-2075.1994.tb06485.x

126. Woldringh, C. L., Grover, N. B., Rosenberger, R. F., & Zaritsky, A. (1980, Oct 7). Dimensional rearrangement of rod-shaped bacteria following nutritional shift-up. II. Experiments with Escherichia coli B/r. *J Theor Biol, 86*(3), 441-454. https://doi.org/10.1016/0022-5193(80)90344-6

127. Yao, Z., Davis, R. M., Kishony, R., Kahne, D., & Ruiz, N. (2012). Regulation of cell size in response to nutrient availability by fatty acid biosynthesis in Escherichia coli. *Proceedings of the National Academy of Sciences, 109*(38), E2561-E2568.

128. Yoshikawa, H., O'Sullivan, A., & Sueoka, N. (1964, Oct). Sequential Replication of the Bacillus Subtilis Chromosome. 3. Regulation of Initiation. *Proc Natl Acad Sci U S A, 52*(4), 973-980. https://doi.org/10.1073/pnas.52.4.973

129. Young, K. D. (2006, Sep). The selective value of bacterial shape. *Microbiol Mol Biol Rev, 70*(3), 660-703. https://doi.org/10.1128/mmbr.00001-06

130. Zheng, H., Bai, Y., Jiang, M., Tokuyasu, T. A., Huang, X., Zhong, F., Wu, Y., Fu, X., Kleckner, N., Hwa, T., & Liu, C. (2020, Aug). General quantitative relations linking cell growth and the cell cycle in Escherichia coli. *Nat Microbiol, 5*(8), 995-1001. https://doi.org/10.1038/s41564-020-0717-x

131. Zheng, H., Ho, P. Y., Jiang, M., Tang, B., Liu, W., Li, D., Yu, X., Kleckner, N. E., Amir, A., & Liu, C. (2016, Dec 27). Interrogating the Escherichia coli cell cycle by cell dimension perturbations. *Proc Natl Acad Sci U S A, 113*(52), 15000-15005. https://doi.org/10.1073/pnas.1617932114

Figure 1

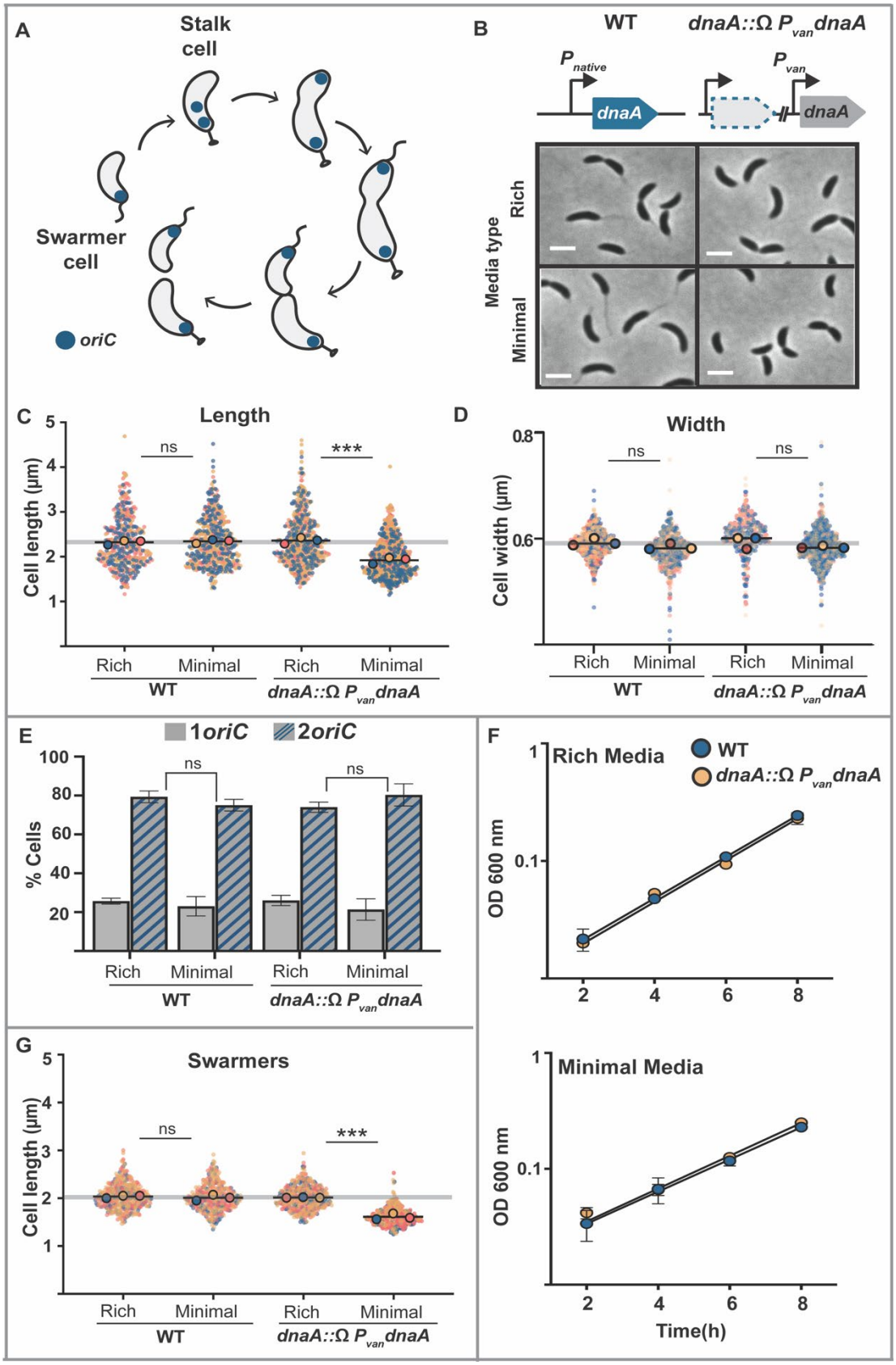
A
Stalk cell
Swarmer cell
oriC
B
WT
dnaA::Ω Pvan dnaA
Pnative
Pvan
dnaA
dnaA
Media type
Rich
Minimal
C
Length
Cell length (µm)
ns
***
Rich
Minimal
Rich
Minimal
WT
dnaA::Ω Pvan dnaA
D
Width
Cell width (µm)
ns
ns
Rich
Minimal
Rich
Minimal
WT
dnaA::Ω Pvan dnaA
E
1oriC
2oriC
% Cells
ns
ns
Rich
Minimal
Rich
Minimal
WT
dnaA::Ω Pvan dnaA
F
Rich Media
WT
dnaA::Ω Pvan dnaA
OD 600 nm
Minimal Media
OD 600 nm
Time(h)
G
Swarmers
Cell length (µm)
ns
***
Rich
Minimal
Rich
Minimal
WT
dnaA::Ω Pvan dnaA

Figure 2

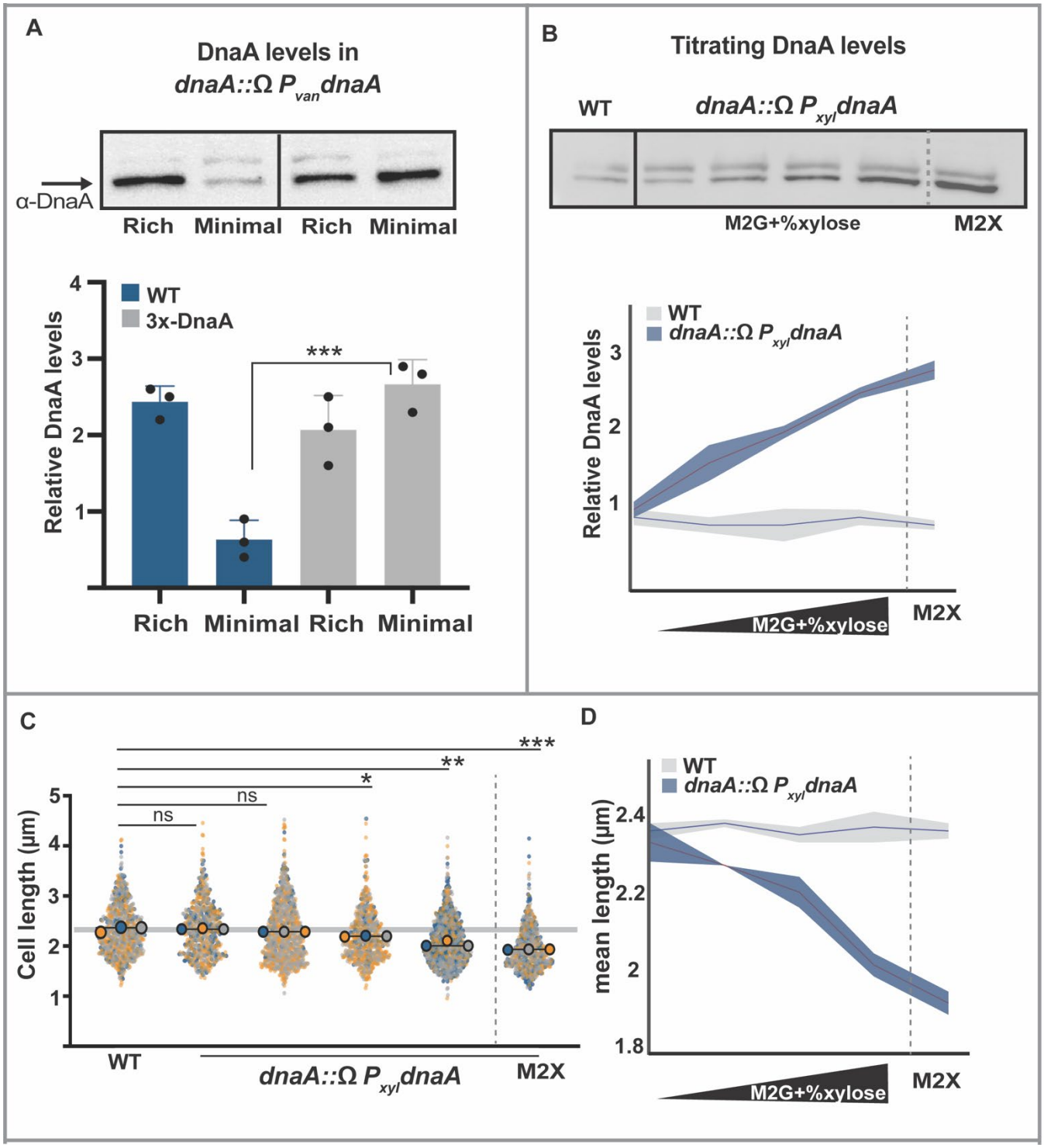
A
DnaA levels in
dnaA::Ω P_van dnaA
α-DnaA
Rich
Minimal
Rich
Minimal
WT
3x-DnaA
Relative DnaA levels
***
Rich
Minimal
Rich
Minimal
B
Titrating DnaA levels
WT
dnaA::Ω P_xyl dnaA
M2G+%xylose
M2X
WT
dnaA::Ω P_xyl dnaA
Relative DnaA levels
M2G+%xylose
M2X
C
***
**
*
ns
ns
Cell length (µm)
WT
dnaA::Ω P_xyl dnaA
M2X
D
WT
dnaA::Ω P_xyl dnaA
mean length (µm)
M2G+%xylose
M2X

Figure 3

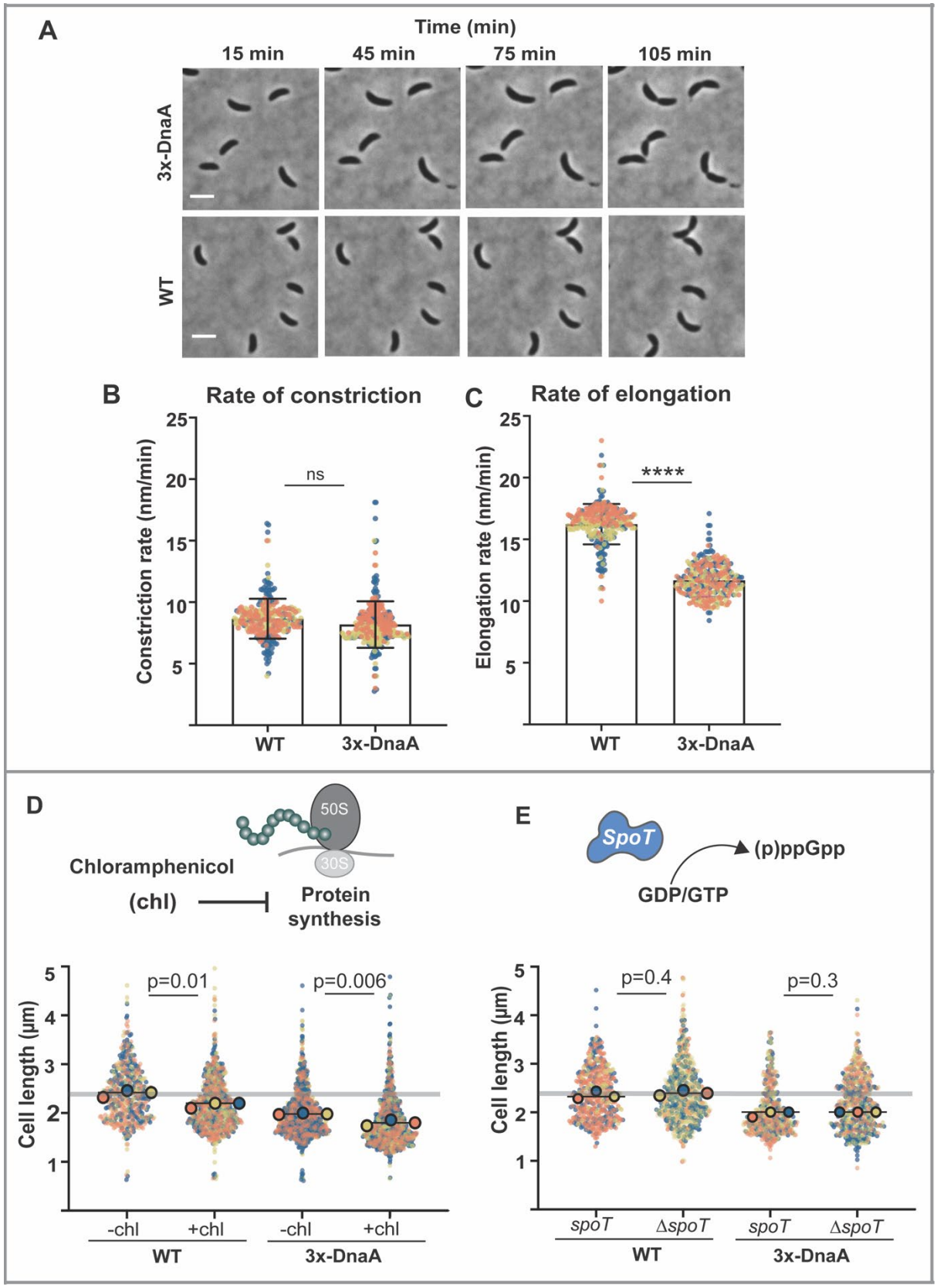
A
Time (min)
15 min
45 min
75 min
105 min
3x-DnaA
WT
B
Rate of constriction
Constriction rate (nm/min)
ns
WT
3x-DnaA
C
Rate of elongation
Elongation rate (nm/min)
****
WT
3x-DnaA
D
50S
30S
Chloramphenicol
(chl)
Protein synthesis
Cell length (µm)
p=0.01
p=0.006
-chl
+chl
-chl
+chl
WT
3x-DnaA
E
SpoT
(p)ppGpp
GDP/GTP
Cell length (µm)
p=0.4
p=0.3
spoT
ΔspoT
spoT
ΔspoT
WT
3x-DnaA

Figure 4

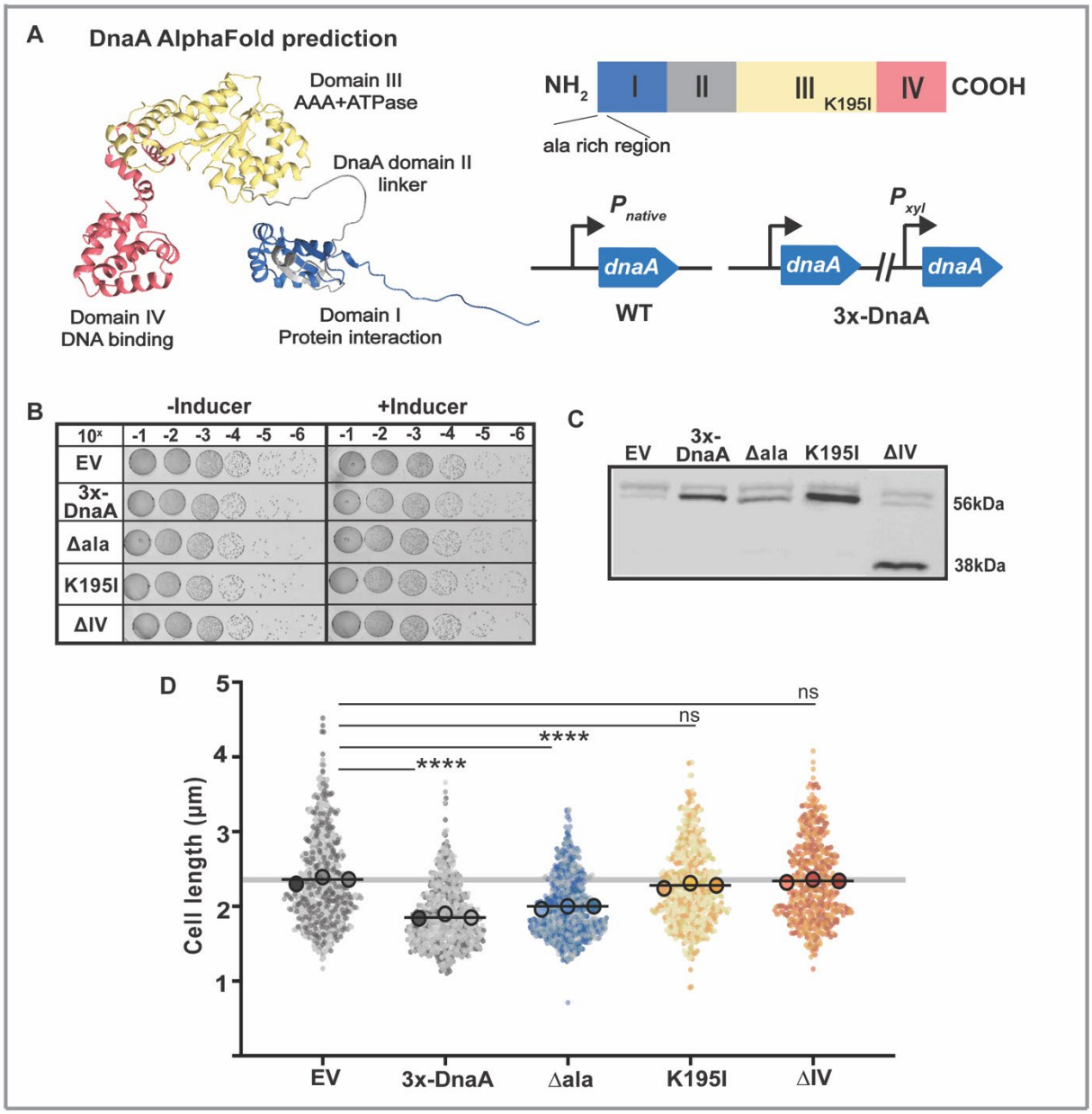
A
DnaA AlphaFold prediction
Domain III
AAA+ATPase
DnaA domain II
linker
Domain IV
DNA binding
Domain I
Protein interaction
NH2
I
II
III
K195I
IV
COOH
ala rich region
Pnative
dnaA
WT
Pxyl
dnaA
dnaA
3x-DnaA
B
-Inducer
+Inducer
10x
-1 -2 -3 -4 -5 -6
-1 -2 -3 -4 -5 -6
EV
3x-DnaA
Δala
K195I
ΔIV
C
EV
3x-DnaA
Δala
K195I
ΔIV
56kDa
38kDa
D
Cell length (µm)
5
4
3
2
1
ns
ns
****
****
EV
3x-DnaA
Δala
K195I
ΔIV

Figure 5

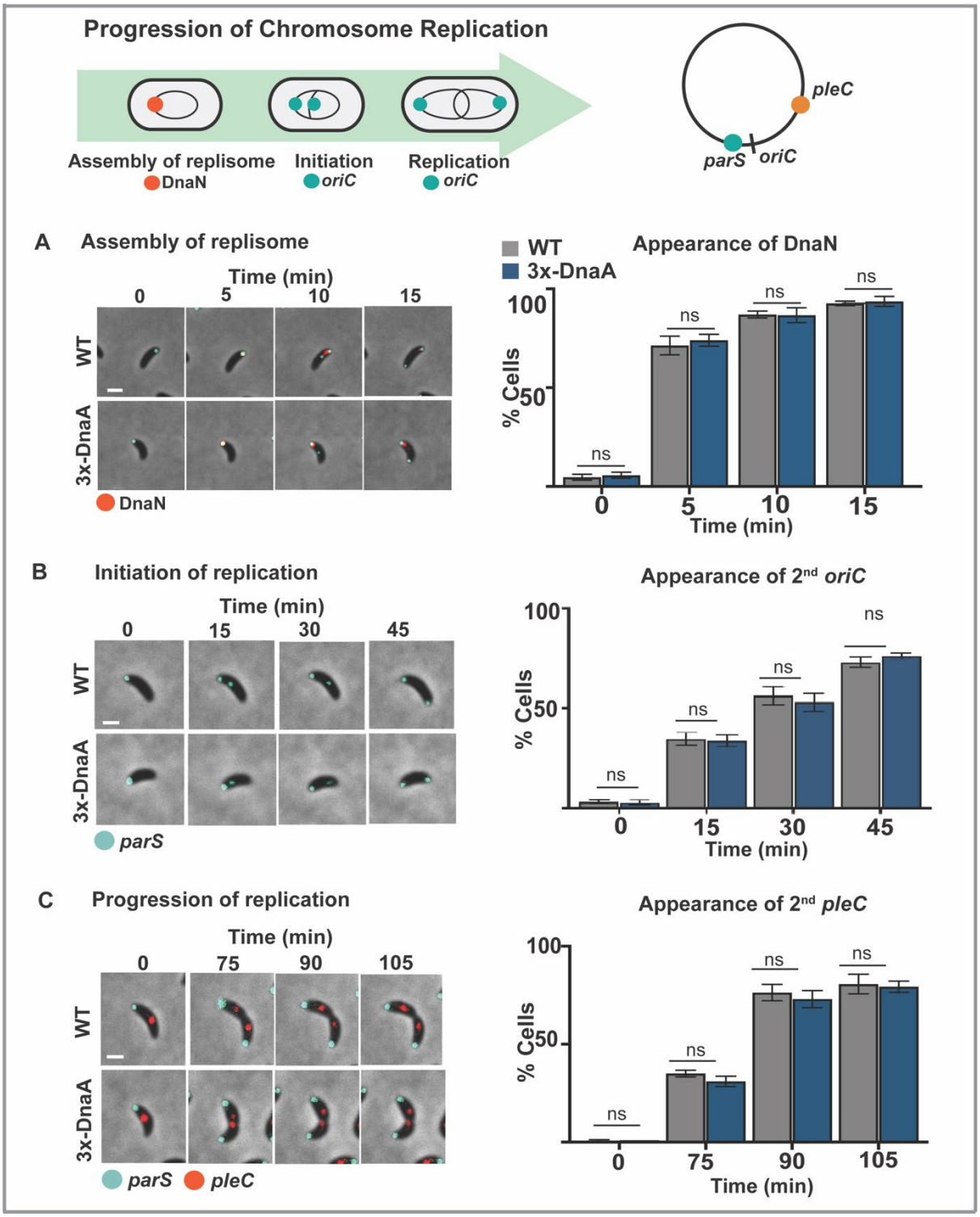
Progression of Chromosome Replication
Assembly of replisome
DnaN
Initiation
oriC
Replication
oriC
pleC
parS
oriC
A
Assembly of replisome
Time (min)
0
5
10
15
WT
3x-DnaA
DnaN
WT
3x-DnaA
Appearance of DnaN
% Cells
100
50
ns
Time (min)
B
Initiation of replication
Time (min)
0
15
30
45
parS
Appearance of 2nd oriC
C
Progression of replication
Time (min)
0
75
90
105
parS
pleC
Appearance of 2nd pleC

Figure 6

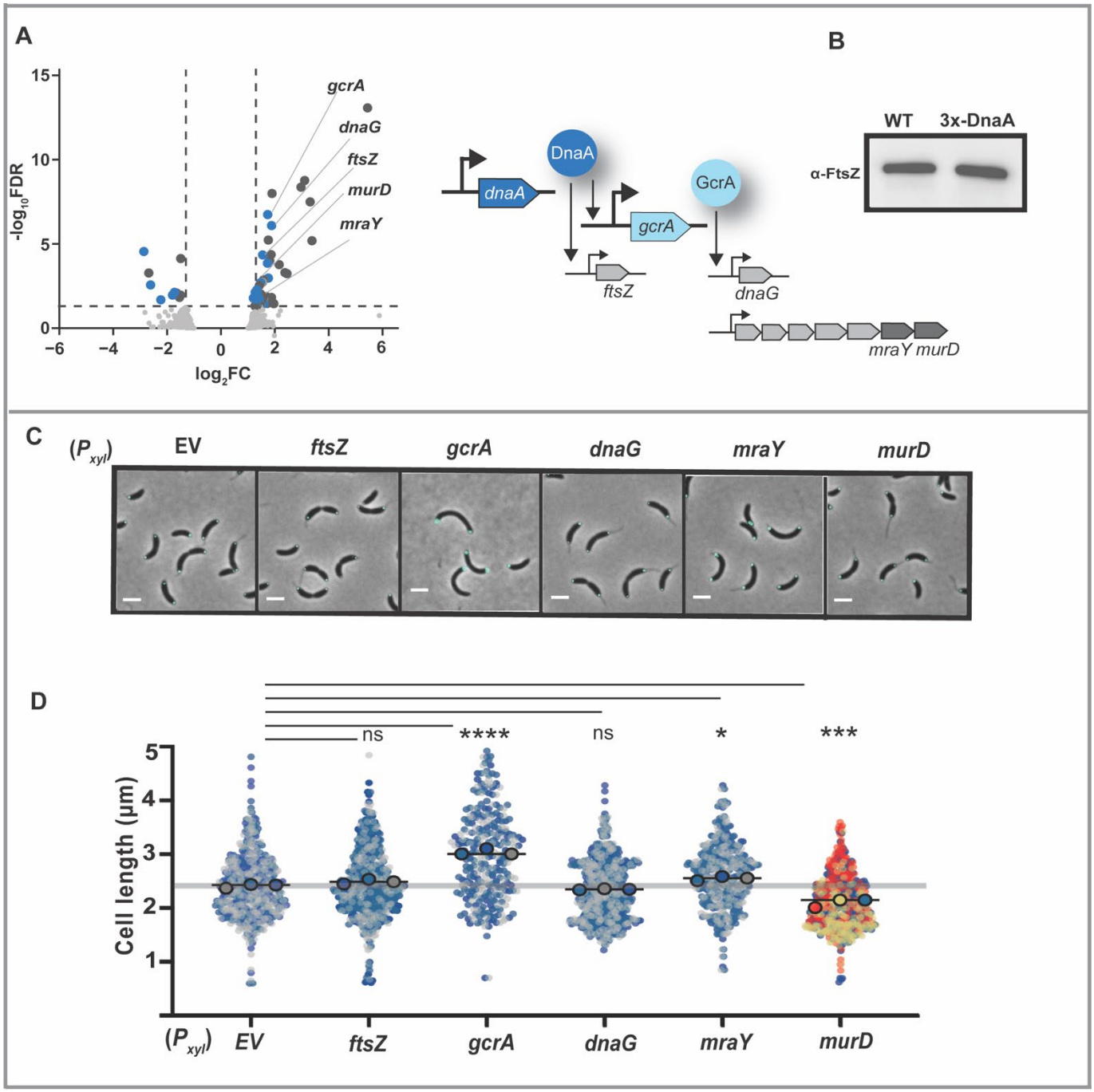
A
B
gcrA
dnaG
ftsZ
murD
mraY
-log10FDR
log2FC
DnaA
GcrA
dnaA
gcrA
ftsZ
dnaG
mraY murD
WT
3x-DnaA
α-FtsZ
C
(Pxyl)
EV
ftsZ
gcrA
dnaG
mraY
murD
D
ns
****
ns
*
***
Cell length (µm)
(Pxyl)
EV
ftsZ
gcrA
dnaG
mraY
murD

Figure 7

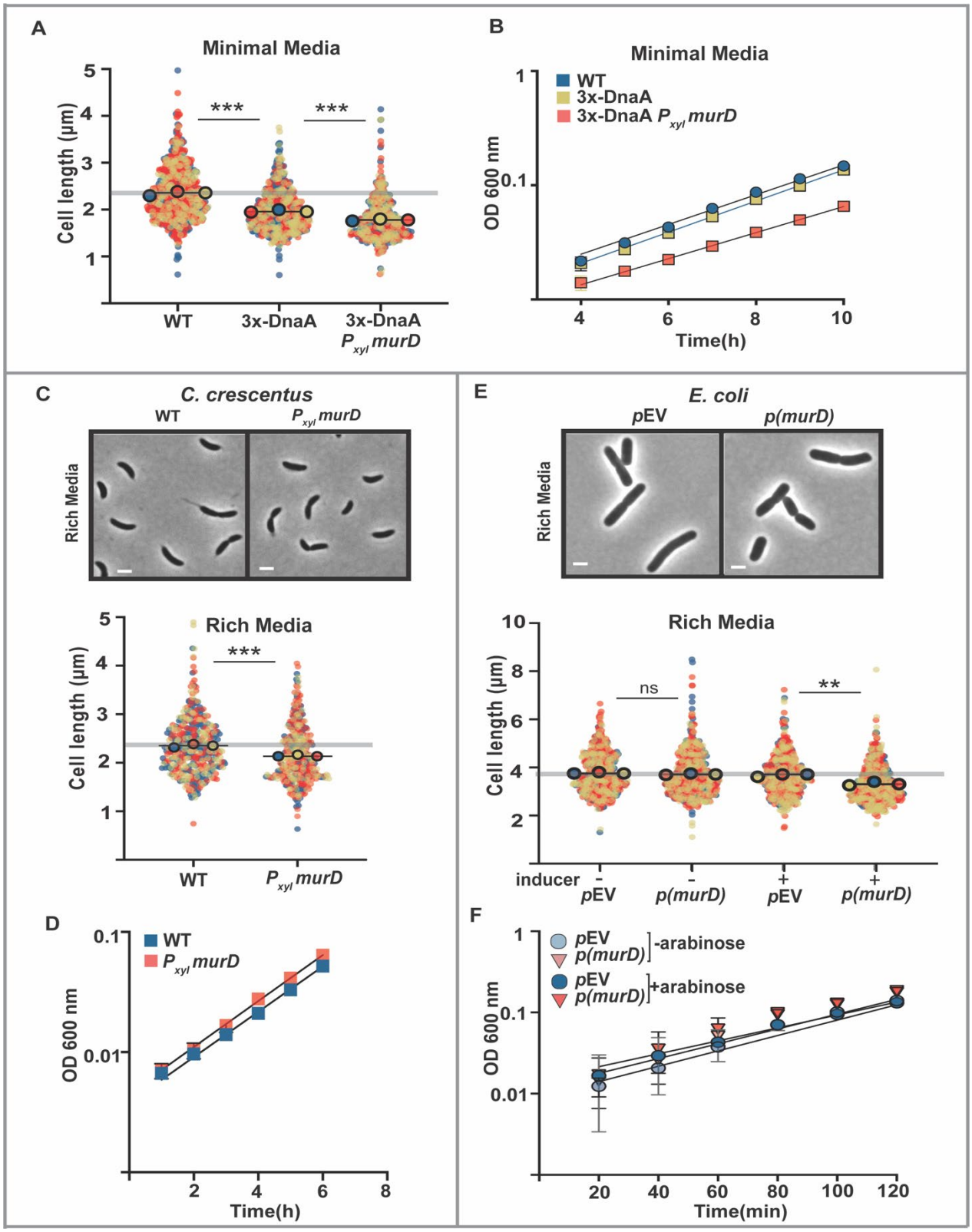
A
Minimal Media
Cell length (µm)
***
***
WT
3x-DnaA
3x-DnaA P_{xyl} murD
B
Minimal Media
WT
3x-DnaA
3x-DnaA P_{xyl} murD
OD 600 nm
Time(h)
C
C. crescentus
WT
P_{xyl} murD
Rich Media
Rich Media
***
Cell length (µm)
WT
P_{xyl} murD
D
WT
P_{xyl} murD
OD 600 nm
Time(h)
E
E. coli
pEV
p(murD)
Rich Media
Rich Media
ns
**
Cell length (µm)
inducer
pEV
p(murD)
pEV
p(murD)
F
pEV
p(murD)
-arabinose
pEV
p(murD)
+arabinose
OD 600 nm
Time(min)

Table 1. RNA-seq data 3x-DnaA vs. DnaA-K195I

Gene ID	Symbol	FC	FDR	Description
CCNA_02793	*NA*	3.3	1.60E-10	S9 family peptidase
CCNA_02792	*NA*	3.1	7.27E-12	TonB-dependent outer membrane receptor
CCNA_03227	*NA*	1.9	1.52E-02	TonB-dependent receptor
CCNA_03144	***dnaG***	1.8	7.54E-07	DNA primase
CCNA_02328	***gcrA***	1.8	3.56E-07	cell cycle sigma 70 cofactor GcrA
CCNA_02891	*NA*	1.7	1.21E-02	GanA-family beta-galactosidase
CCNA_02976	*NA*	1.7	3.46E-02	MCP-signal associated domain protein
CCNA_02640	***mraY***	1.6	1.63E-02	phospho-N-acetylmuramoyl-pentapeptide-transferase
CCNA_03270	*NA*	1.6	3.53E-02	AsnC-family transcriptional regulator
CCNA_02902	*NA*	1.5	1.89E-03	xylan alpha-1,2-glucuronosidase
CCNA_01485	*NA*	1.5	2.18E-02	aldose 1-epimerase
CCNA_01486	*NA*	1.5	1.93E-02	GguC-family protein
CCNA_02639	***murD***	1.5	1.99E-03	UDP-N-acetylmuramoylalanine--D-glutamate ligase
CCNA_02623	***ftsZ***	1.5	6.00E-05	cell division protein FtsZ
CCNA_01003	*fliO*	1.5	3.48E-02	flagellar biosynthesis protein FliO
CCNA_01979	*lexA*	1.5	3.46E-02	LexA repressor
CCNA_01116	*divJ*	1.5	9.31E-03	histidine protein kinase DivJ
CCNA_01489	*abfA*	1.5	3.37E-02	alpha-L-arabinofuranosidase
CCNA_03105	*NA*	-1.5	1.09E-02	DnaJ domain protein
CCNA_02814	*NA*	-1.5	1.52E-02	transposase
CCNA_03426	*NA*	-1.8	1.09E-02	MarR family repressor protein
CCNA_01247	*NA*	-2.6	2.74E-03	CESA-like glycosyltransferase
CCNA_03231	*relB-4*	-2.9	2.85E-05	anti-toxin protein relB-4